Cetus) was set at 95 °C for 30 s, 55 °C for 1 min and 72 °C for 1 min. After amplification for 15, 20, 25, 30, 35 and 40 cycles, 10 μl of each sample was electrophoresed in 3.0% NuSieve 3:1 agarose (FMC BioProducts) and transferred to nylon membranes. Oligonucleotides corresponding to each of the PCR products for bovine ECE-1 and GAPDH (Table 1) were synthesized as internal probes, 5′-end labeled by [γ-^{32}P]dATP (Amersham), and hybridized to the membranes. The membranes were washed in 0.3 × SSC at 55 °C and exposed to an imaging plate (Fuji Photo Film). The radioactivity of each band was quantified with a BAS 2000 (Fuji). ECE-1 mRNA levels were compared between samples by the calculation of relative ratios using corresponding GAPDH mRNA levels.

2.4. Measurement of ET-1 and big ET-1 concentrations in culture media

Detection of ET-1 and big ET-1 in the medium with ECs subjected to shear stress was conducted using an ELISA assay (Diagnostica Stago). The color reaction was performed with TBM substrate and measured at 450 nm using a microplate reader.

2.5. Analysis of peroxide production by flow cytometry

Peroxide production of ECs subjected to shear stress or static culture was analyzed using 2′,7′-dichlorofluorescin diacetate (DCFH-DA) by cytometry. Subsequent to static or shear stress treatment with DCFH-DA for a suitable period, ECs were washed with PBS twice, treated with buffer containing EDTA and scraped from the plate. ECs were centrifuged at 500 × *g* for 5 min at 4 °C and the supernatant fluid was aspirated. Pellets were resuspended in PBS, washed and fixed with paraformaldehyde in PBS at a final concentration of 1% (wt/vol). The relative fluorescence intensities were quantified using flow cytometry in a fluorescence-activated cell sorter (FACScan IV, Becton Dickinson) with absorption set at 488 nm and the detector set at 530 nm.

2.6. Statistical analysis

Results are expressed as the mean ± S.D. of at least three independent experiments. Significance was determined by using Student's *t* test, and the level of statistical significance was defined as $P<0.05$.

3. Results

3.1. Effect of shear stress on ECE-1 and ET-1 mRNA expression in BAECs and HUVECs

As shown in Fig. 1a, the application of a relatively low shear stress (1.5 dyn/cm^2), comparable to that present in veins, apparently attenuated the mRNA expressions of ECE-1 and ET-1 in BAECs. The application of a moderately high shear stress (15 dyn/cm^2) similar to that observed in arteries further attenuated the expression of both mRNAs. The application of shear stress did not affect the mRNA expression of GAPDH. The mRNA of ECE-1 was attenuated to 15% of the control, at a shear stress of 15 dyn/cm^2 for 24 h (Fig. 1b).

To examine shear stress-regulated expression of the ECE-1 gene in endothelial cells from the tissues of different species, we examined the effect of shear stress on the mRNA expression of the ECE-1 subtypes in HUVECs. ECE-1b mRNA could not be detected in HUVECs even after 50 cycles of amplification. As was the case for BAECs, shear stress (5–25 dyn/cm^2) attenuated the mRNA expression of ECE-1 and its subtype ECE-1a in an intensity-dependent manner (Fig. 1c).

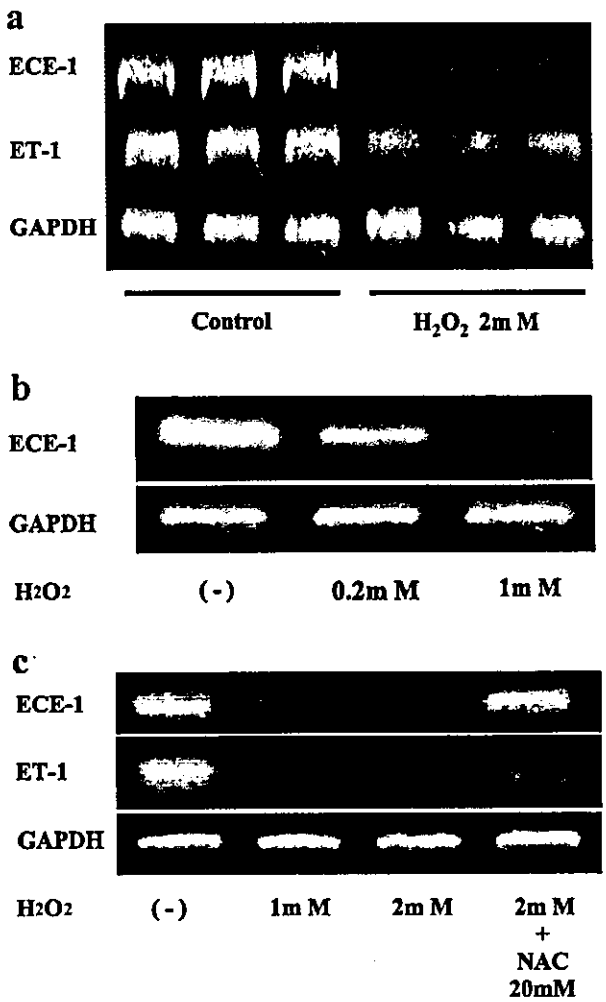

Fig. 3. Attenuation of ECE-1 and ET-1 mRNA expressions by H_2O_2. (a) RT-PCR analysis of ECE-1 and ET-1 mRNA expressions in BAECs in the presence or absence of 2.0 mM H_2O_2 for 6 h. (b) RT-PCR analysis of dose-dependent effect of H_2O_2 on ECE-1 mRNA expression in BAECs 6 h after the addition. (c) RT-PCR analysis of the effect of NAC (20 mM) on down-regulation of ECE-1 and ET-1 mRNA expressions in BAECs by H_2O_2.

As shown in Fig. 1d, ECE-1 and ET-1 mRNA expressions under a shear stress of 15 dyn/cm^2 were down-regulated in proportion to time from 1 to 24 h.

3.2. Effect of shear stress on ET-1 and big ET-1 concentrations in BAECs

As shown in Table 2, 4 h after the exposure to shear stress, there was no significant difference between 1.5 and 15 dyn/cm^2 in the peptide level of ET-1 or big ET-1 in the media of BAECs; however, 8 or 12 h after the onset of flow, a significant reduction in the peptide level of both ET-1 and big ET-1 was observed at a shear stress of 15 dyn/cm^2, compared with 1.5 dyn/cm^2.

3.3. Shear stress increases intracellular peroxide production in endothelial cells

We also examined the production of intracellular peroxides in sheared BAECs as early as 30 min after the onset of flow. As shown in Fig. 2, exposure to a shear stress of 15 dyn/cm^2 for 30 min increased intracellular peroxide production in ECs compared with the static control. The levels of intracellular peroxides in sheared ECs were comparable to those in static ECs treated with 0.2 mM H_2O_2 for 30 min. Furthermore, the increase in the level of intracellular peroxides in both sheared ECs and static ECs treated with 0.2 mM H_2O_2 was abolished in the presence of 20 mM NAC, with return to control levels.

3.4. Effect of H_2O_2 on ECE-1 and ET-1 mRNA expressions in static culture

We have previously shown that in H_2O_2-treated BAECs, both the ET-1 mRNA level and the ET-1 concentration are attenuated in proportion to the concentration of H_2O_2 [16]. This time, to further investigate the effect of H_2O_2 on the ECE-1 mRNA expression of BAECs in static culture, we added H_2O_2 (0.2–2.0 mM) to the culture medium. ECE-1 as well as ET-1 mRNA expression was significantly and dose-dependently attenuated in the presence of H_2O_2 (Fig. 3a–c). The down-regulation of ET-1 and ECE-1 mRNAs by H_2O_2 (2 mM) was inhibited with addition of 20 mM NAC (Fig. 3c).

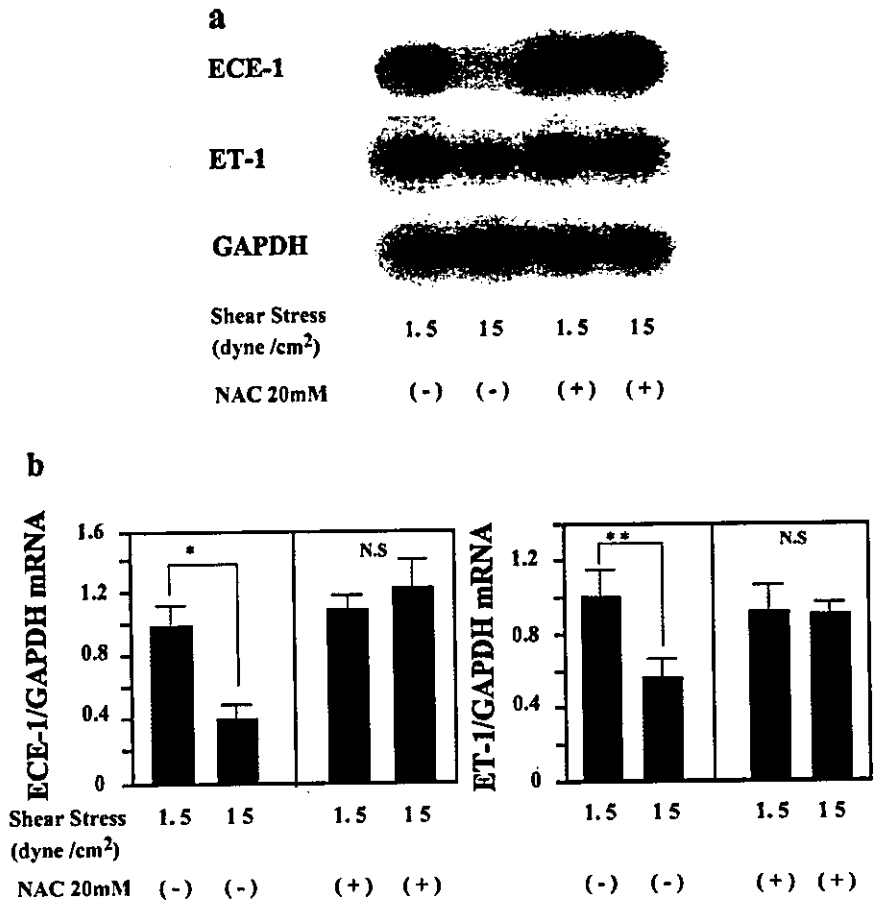

Fig. 4. Effects of NAC on down-regulation of ECE-1 and ET-1 mRNA expressions by shear stress. (a) RT-PCR and Southern blotting of ECE-1 and ET-1 mRNA expressions at the shear stress of 1.5 dyn/cm^2 and 15 dyn/cm^2 in the absence and presence of NAC (20 mM) for 12 h. (b) Quantitative analysis of down-regulation of ECE-1 and ET-1 mRNA expressions by shear stress and the effect of 20 mM NAC. *$P<0.05$; **$P<0.01$.

3.5. Effect of the antioxidant on the shear stress-induced attenuation of ECE-1 and ET-1 mRNA expression

Fig. 4a illustrates the effects of the antioxidant NAC on the shear stress-induced ECE-1 and ET-1 mRNA expression. As demonstrated above, a moderately strong shear stress (15 dyn/cm^2) clearly elicited an attenuation of the ECE-1 and ET-1 mRNA expressions, compared with 1.5 dyn/cm^2, in the absence of NAC. However, in the presence of 20 mM NAC, the attenuation induced by 15 dyn/cm^2 shear stress was almost completely abolished. Fig. 4b presents the results of a quantitative analysis of the down-regulation of ECE-1 and ET-1 mRNA expression by shear stress and its abolishment with 20 mM NAC.

4. Discussion

We previously demonstrated that physiological laminar shear stress up-regulates the mRNA expression and secretion of two novel endothelium-derived vasorelaxing peptides, CNP and AM [6]. In contrast, it has been reported that shear stress loading decreases the concentration of ET in cultured medium [9]. In a previous study, we demonstrated that ECE-1 as well as ET-1 mRNA expression was attenuated in proportion to the intensity of the shear stress for 24 h [17]. In the present study, we confirmed that ECE-1 mRNA expression was attenuated by shear stress in an intensity- and a time-dependent manner both in BAECs and in HUVECs. We also confirmed that in HUVECs, the mRNA expression of ACE was attenuated by shear stress in parallel with that of ECE-1, which was consistent with another report [18]. The down-regulation of ECE-1 mRNA as well as ET-1 mRNA by shear stress was reflected in the coordinated decrease in the protein level of ET-1 and big ET-1.

Recently, it has been reported that shear stress increases ROS levels in shear-treated ECs [15]. In the present study, we confirmed that shear stress induced the production of intracellular peroxides in BAECs. To further examine the effect of an increase in ROS on the mRNA of ECE-1 and ET-1, we exposed BAECs to H_2O_2, and found the expression of ECE-1 and ET-1 mRNA to be reduced in response to H_2O_2. This result is compatible with our previous work to show that oxidative stress suppresses endothelin secretion [16]. Furthermore, the down-regulation of ECE-1 and ET-1 mRNA expressions by shear stress was significantly attenuated by treatment with the antioxidant NAC. These findings suggest that the shear stress-induced reductions in ECE-1 and ET-1 expression are mediated through the activation of oxidative stress.

We previously demonstrated that the endothelial secretions of CNP and AM are augmented by shear stress in a time- and intensity-dependent manner, and furthermore, that the expression of CNP and AM at both mRNA and peptide levels is augmented in proportion to the concentration of H_2O_2 in BAECs [19]. The augmentations of CNP and AM by both shear stress and oxidative stress are consistent with attenuations of ECE-1 and ET-1 expressions caused by both of these stresses in the present study.

Recently, the importance of the shear stress responsive element (SSRE) for shear stress-induced transcriptional gene regulation has been described. SSRE was originally reported to be 5′-GAGACC-3′ in the promoter of platelet-derived growth factor-B (PDGF-B) chain as a positive regulatory element and confirmed to confer shear stress responsiveness [20]. This element is also found in the 5′ promoter region of other shear stress-inducible genes such as the endothelial nitric oxide (NO) synthase [21], tissue plasminogen activator (tPA) [20] and transforming growth factor-β1 (TGF-β1) genes [20]. Moreover, other SSREs have been identified such as a 5′-TGACTCC-3′ sequence coupled to the transcription factor AP-1 in the promoter of monocyte chemotacting protein-1 (MCP-1) [22], a 5′-GCGGGGGCGGGG-3′ sequence coupled to SP-1 in the promoter of tissue factor (TF) [23], and a double 5′-TG-ACTCA-3′ sequence coupled to c-*jun* in the promoter of vascular cell adhesion molecule-1 (VCAM-1) [24]. In human ECE-1 genes, there are four copies of the 5′-GAG-ACC-3′ element, −3347, −3167, −2746 and −602 bp, respectively, upstream of the putative transcription initiation point. However, the other SSREs are not present in human ECE-1 genes.

The NF-kappaB-dependent signal transduction for the regulation of gene expression in endothelial cells has been demonstrated to be mediated through binding to the element 5′-GAGACC-3′ [25]. Recently, it has been also reported that the p38 mitogen-activated protein (MAP) kinase regulates NF-kappaB-dependent gene transcription under specific conditions [26]. P38 MAP kinase, as well as NF-kappaB, has been reported to be stress-activated and rapidly up-regulated after treatment with H_2O_2 [27]. Therefore, it may be the case that shear stress-induced intracellular reactive oxygen free radicals transduce the signal that leads to the activation of p38 MAP kinase, which regulates ECE-1 promoter activity through the transcription factor NF-kappaB. Gene regulation of the activation of NF-kappaB induced by ROS was reported, however, to augment gene expression [28,29]. The mechanism behind the negative regulation of ECE-1 gene expression by shear stress via the increase in ROS observed in the present study needs to be investigated further.

There are accumulating studies to demonstrate that many cardiovascular diseases, such as arterial and pulmonary hypertension, atherosclerosis, congestive heart failure and renal failure, are associated with local activation of the endothelin system [30]. Thus, the therapeutic potential of endothelin receptor antagonists in cardiovascular disease is indicated. In these disorders, the decrease in endothelial shear stress plays the pathophysiological role. Regulatory mechanism of the endothelin system by shear stress observed in the present study should therefore be of clinical relevance.

In conclusion, we have demonstrated that physiological shear stress down-regulates the mRNA expression of ECE-1 as well as ET-1, through an increase in oxidative stress in endothelial cells. This, along with our previous findings on the effect of shear stress on the expression of endothelium-derived relaxing substances, suggests that the coordinated regulation of the production of endothelium-derived vasoactive substances by shear stress serves to maintain vascular tone and proliferation within a certain range and protect vascular walls from hypertension and atherosclerosis.

Acknowledgements

This work was supported in part by research grants from the Japanese Ministry of Education, Science and Culture; Japanese Society for the promotion of 'Science Research for the Future' program (JSPS-RFTF 96100204, JSPS-RFTF 98L00801); and Japan Smoking Research Foundation.

References

[1] Malek AM, Izumo S. Molecular aspects of signal transduction of shear stress in the endothelial cell. J Hypertens 1994;12:989–99.
[2] Zarins CK, Giddens DP, Bharadvaj BK, Sottiurai VS, Mabon RF, Glagov S. Carotid bifurcation atherosclerosis. Quantitative correlation of plaque localization with flow velocity profiles and wall shear stress. Circ Res 1983;53:502–14.
[3] Itoh H, Mukoyama M, Pratt RE, Gibbons GH, Dzau VJ. Multiple autocrine growth factors modulate vascular smooth muscle cell growth response to angiotensin II. J Clin Invest 1993;91:2268–74.
[4] Itoh H, Pratt RE, Dzau VJ. Atrial natriuretic polypeptide inhibits hypertrophy of vascular smooth muscle cells. J Clin Invest 1990; 86:1690–7.
[5] Suga S, Nakao K, Itoh H, Komatsu Y, Ogawa Y, Hama N, et al. Endothelial production of C-type natriuretic peptide and its marked augmentation by transforming growth factor-beta. Possible existence of "vascular natriuretic peptide system". J Clin Invest 1992;90: 1145–9.
[6] Chun TH, Itoh H, Ogawa Y, Tamura N, Takaya K, Igaki T, et al. Shear stress augments expression of C-type natriuretic peptide and adrenomedullin. Hypertension 1997;29:1296–302.
[7] Kitamura K, Kangawa K, Kawamoto M, Ichiki Y, Nakamura S, Matsuo H, et al. Adrenomedullin: a novel hypotensive peptide isolated from human pheochromocytoma. Biochem Biophys Res Commun 1993;192:553–60.
[8] Sugo S, Minamino N, Kangawa K, Miyamoto K, Kitamura K, Sakata J, et al. Endothelial cells actively synthesize and secrete adrenomedullin. Biochem Biophys Res Commun 1994;201:1160–6.
[9] Malek A, Izumo S. Physiological fluid shear stress causes downregulation of endothelin-1 of mRNA in bovine aortic endothelium. Am J Physiol 1992;263:C389–96.
[10] Xu D, Emoto N, Giaid A, Slaughter C, Kaw S, deWit D, et al. ECE-1: a membrane-bound metalloprotease that catalyzes the proteolytic activation of big endothelin-1. Cell 1994;78:473–85.
[11] Emoto N, Yanagisawa M. Endothelin-converting enzyme-2 is a membrane-bound, phosphoramidon-sensitive metalloprotease with acidic pH optimum. J Biol Chem 1995;270:15262–8.
[12] Corder R, Khan N, Harrison VJ. A simple method for isolation human endothelin converting enzyme free from contamination by neutral endopeptidase 24.11. Biochem Biophys Res Commun 1995;207: 355–62.
[13] Valdenaire O, Rohrbacher E, Mattei MG. Organization of the gene encoding the human endothelin-converting enzyme (ECE-1). J Biol Chem 1995;270:29794–8.
[14] Shimada K, Takahashi M, Ikeda M, Tanzawa K. Identification and characterization of two isoforms of an endothelin-converting enzyme-1. FEBS Lett 1995;371:140–4.
[15] Chiu JJ, Wung BS, Shyy JY, Hsieh HJ, Wang DL. Reactive oxygen species are involved in shear stress-induced intercellular adhesion molecule-1 expression in endothelial cells. Arterioscler Thromb Vasc Biol 1997;17:3570–7.
[16] Saito T, Itoh H, Chun T-H, Fukunaga Y, Yamashita J, Doi K, et al. Coordinate regulation of endothelin and adrenomedullin secretion by oxidative stress in endothelial cells. Am J Physiol 2001;281: H1364–71.
[17] Masatsugu K, Itoh H, Chun T-H, Ogawa Y, Tamura N, Yamashita J, et al. Physiologic shear stress suppresses endothelin-converting enzyme-1 expression in vascular endothelial cells. J Cardiovasc Pharmacol 1998;31:S42–5.
[18] Rieder MJ, Carmona R, Krieger JE, Pritchard Jr KA, Greene AS. Suppression of angiotensin-converting enzyme expression and activity by shear stress. Circ Res 1997;80:312–9.
[19] Chun T-H, Itoh H, Saito T, Yamahara K, Doi K, Mori Y, et al. Oxidative stress augments secretion of endothelium-derived relaxing peptide, C-type natriuretic peptide and adrenomedullin. Oxidative stress augments secretion of endothelium-derived relaxing peptides, C-type natriuretic peptide and adrenomedulin. J Hypertens 2000; 18:575–80.
[20] Resnick N, Collins T, Atkinson W, Bonthron DT, Dewey Jr CF, Gimbrone Jr MA. Platelet-derived growth factor B chain promoter contains a *cis*-acting fluid shear-stress-responsive element. Proc Natl Acad Sci U S A 1993;90:4591–5.
[21] Nunokawa Y, Ishida N, Tanaka S. Promoter analysis of human inducible nitric oxide synthase gene associated with cardiovascular homeostasis. Biochem Biophys Res Commun 1994;200:802–7.
[22] Shyy JY, Lin MC, Han J, Lu Y, Petrime M, Chien S. The *cis*-acting phorbol ester "12-*O*-tetradecanoylphorbol 13-acetate"-responsive element is involved in shear stress-induced monocyte chemotactic protein 1 gene expression. Proc Natl Acad Sci U S A 1995;92:8069–73.
[23] Lin MC, Almus-Jacobs F, Chen HH, Parry GC, Mackman N, Shyy JY, et al. Shear stress induction of the tissue factor gene. J Clin Invest 1997;99:737–44.
[24] Korenaga R, Ando J, Kosaki K, Isshiki M, Takada Y, Kamiya A. Negative transcriptional regulation of the VCAM-1 gene by fluid shear stress in murine endothelial cells. Am J Physiol 1997;273: C1506–15.
[25] Khachigian LM, Resnick N, Gimbrone Jr MA, Collins T. Nuclear factor-kappa B interacts functionally with the platelet-derived growth factor B-chain shear-stress response element in vascular endothelial cells exposed to fluid shear stress. J Clin Invest 1995;96:1169–75.
[26] Carter AB, Knudtson KL, Monick MM, Hunninghake GW. The p38 mitogen-activated protein kinase is required for NF-kappaB-dependent gene expression. The role of TATA-binding protein (TBP). J Biol Chem 1999;274:30858–63.
[27] Huot J, Houle F, Marceau F, Landry J. Oxidative stress-induced actin reorganization mediated by the p38 mitogen-activated protein kinase/heat shock protein 27 pathway in vascular endothelial cells. Circ Res 1997;80:383–92.
[28] Lee KS, Buck M, Houglum K, Chojkier M. Activation of hepatic stellate cells by TGF alpha and collagen type I is mediated by oxidative stress through c-myb expression. J Clin Invest 1995;96:2461–8.
[29] Pueyo ME, Gonzalez W, Nicoletti A, Savoie F, Amal JF, Michel JB. Angiotensin II stimulates endothelial vascular cell adhesion molecule-1 via nuclear factor-kappa B activation induced by intracellular oxidative stress. Arterioscler Thromb Vasc Biol 2000;20:645–51.
[30] Luscher TF, Barton M. Endothelins and endothelin receptor antagonists. Therapeutic considerations for a novel class of cardiovascular drugs. Circulation 2000;102:2432–40.

Significance and therapeutic potential of the natriuretic peptides/cGMP/cGMP-dependent protein kinase pathway in vascular regeneration

Kenichi Yamahara*, Hiroshi Itoh*†, Tae-Hwa Chun*, Yoshihiro Ogawa*, Jun Yamashita*, Naoki Sawada*, Yasutomo Fukunaga*, Masakatsu Sone*, Takami Yurugi-Kobayashi*, Kazutoshi Miyashita*, Hirokazu Tsujimoto*, Hyun Kook‡, Robert Feil§, David L. Garbers¶, Franz Hofmann§, and Kazuwa Nakao*

*Department of Medicine and Clinical Science, Kyoto University Graduate School of Medicine, Kyoto 606-8507, Japan; ‡Research Institute of Medical Sciences, Chonnan National University Medical School, Gwangju 501-746, Republic of Korea; §Institut für Pharmakologie und Toxikologie, Technische Universität München, Munich 80802, Germany; ¶Cecil H. and Ida Green Center for Reproductive Biology Sciences, Howard Hughes Medical Institute, Department of Pharmacology, University of Texas Southwestern Medical Center, Dallas, TX 75390

Contributed by David L. Garbers, December 31, 2002

Natriuretic peptides (NPs), which consist of atrial, brain, and C-type natriuretic peptides (ANP, BNP, and CNP, respectively), are characterized as cardiac or vascular hormones that elicit their biological effects by activation of the cGMP/cGMP-dependent protein kinase (cGK) pathway. We recently reported that adenoviral gene transfer of CNP into rabbit blood vessels not only suppressed neointimal formation but also accelerated reendothelialization, a required step for endothelium-dependent vasorelaxation and antithrombogenicity. Accordingly, we investigated the therapeutic potential of the NPs/cGMP/cGK pathway for vascular regeneration. In transgenic (Tg) mice that overexpress BNP in response to hindlimb ischemia, neovascularization with appropriate mural cell coating was accelerated without edema or bleeding, and impaired angiogenesis by the suppression of nitric oxide production was effectively rescued. Furthermore, in BNP-Tg mice, inflammatory cell infiltration in ischemic tissue and vascular superoxide production were suppressed compared with control mice. Ischemia-induced angiogenesis was also significantly potentiated in cGK type I Tg mice, but attenuated in cGK type I knockout mice. NPs significantly stimulated capillary network formation of cultured endothelial cells by cGK stimulation and subsequent Erk1/2 activation. Furthermore, gene transfer of CNP into ischemic muscles effectively accelerated angiogenesis. These findings reveal an action of the NPs/cGMP/cGK pathway to exert multiple vasculoprotective and regenerative actions in the absence of apparent adverse effects, and therefore suggest that NPs as the endogenous cardiovascular hormone can be used as a strategy of therapeutic angiogenesis in patients with tissue ischemia.

Natriuretic peptides (NPs) consist of atrial NP (ANP), brain NP (BNP), and C-type NP (CNP). They share the same intracellular signal transduction pathway for cGMP/cGMP-dependent protein kinase (cGK) as nitric oxide (NO). We have demonstrated that ANP and BNP are cardiac hormones that are produced mainly in the atrium and ventricle, respectively (1, 2). CNP, in contrast, is produced in and secreted from endothelial cells (ECs) to act as a local regulator of vascular tone and growth (3).

We recently reported that in both rabbit balloon injury and vein graft models, overexpression of the CNP gene by adenoviral vector accelerated reendothelialization and inhibited vascular smooth muscle proliferation (4, 5). This finding indicates the complex responses to NPs in different types of vascular cells, both ECs and smooth muscle cells (SMCs).

A large body of literature indicates an essential role of endothelial NO for angiogenesis. Previous studies demonstrated that vascular endothelial growth factor (VEGF) stimulates Akt/protein kinase B (6, 7), which has been shown to phosphorylate endothelial NO synthase, leading to its activation (8, 9). VEGF-stimulated proliferation of cultured ECs, triggered by endothelial NO synthase activation (10), was also shown to require intracellular signaling through cGK, Raf-1 kinase, and Erk1/2 (11, 12). Based on these findings, we hypothesized that NPs could promote vascular regeneration. To examine this hypothesis, we used a mouse model of operatively induced hindlimb ischemia (13) to investigate the effects of NPs on angiogenesis by using transgenic (Tg) mice that overexpress BNP (14) with or without N^{ω}-nitro-L-arginine methyl ester (L-NAME), an inhibitor of NO synthase. We also applied this model to both cGK type I (cGKI)-knockout (15) and Tg mice to investigate the impact of cGKI, one of the cGK isoforms, which is present in ECs and SMCs. Finally, we examined the effect of CNP on angiogenesis by a gene-transfer approach to seek the therapeutic potentials of NPs in vascular regeneration. The present study elucidates the action of the NPs/cGMP/cGKI pathway on angiogenesis and provides a strategy for therapeutic angiogenesis by using an endogenous cardiovascular hormone to exert vasculoprotective and vasculoregenerative actions in the absence of apparent adverse effects.

Materials and Methods

BNP-Tg Mice. Generation of BNP-Tg mice (line 55) was reported (14). BNP-Tg showed a marked increase in plasma BNP levels ($1.8 \pm 1.1 \times 10^{-9}$ M) compared with their control littermates (non-Tg) ($<0.06 \times 10^{-9}$ M; refs. 14 and 16). These mice (10–15 wk) were randomly allotted to four treatment groups: BNP-Tg and non-Tg, with or without L-NAME (Nacalai Tesque, Kyoto) administration (200 mg/liter in drinking water; ref. 17).

cGKI-Knockout Mice. We developed mice with targeted disruption of the cGKI gene (15). We used homozygous cGKI mutant mice ($cGKI^{-/-}$), heterozygous mutant mice ($cGKI^{+/-}$), and their control littermates ($cGK^{+/+}$) (10–15 wk).

cGKI-Tg Mice. We generated cGKI-Tg mice (T.-H.C. and H.I., unpublished data). Briefly, the cDNA coding for human cGKIα, which we cloned (18), was subcloned into the expression vector pCXN2 (19), driven by the CAG promoter (pCXN2-hcGKIα). The fragment of pCXN2-hcGKIα was microinjected into a C57BL/6 mouse. We used mice with 15 copies of the transgene and their control littermates at the age of 10–15 wk. To confirm cGKI expression in cGKI-Tg mice, Northern blot analysis was

Abbreviations: NP, natriuretic peptide; ANP, atrial NP; BNP, brain NP; CNP, C-type NP; cGK, cGMP-dependent protein kinase; EC, endothelial cell; SMC, smooth muscle cell; Tg, transgenic; L-NAME, N^{ω}-nitro-L-arginine methyl ester; LDPI, laser Doppler perfusion image; PECAM-1, platelet EC adhesion molecule-1; SMA, smooth muscle actin, GC, guanylyl cyclase; VEGF, vascular endothelial growth factor.

†To whom correspondence should be addressed at: Department of Medicine and Clinical Science, Kyoto University Graduate School of Medicine, 54 Shogoin Kawahara-cho, Sakyo-ku, Kyoto 606-8507, Japan. E-mail: hilto@kuhp.kyoto-u.ac.jp.

www.pnas.org/cgi/doi/10.1073/pnas.0538059100

performed with a human cGKIα-specific probe, a 311-bp-long fragment at the 5' end sequence released by pCXN2-hcGKIα.

Ligation Model. After being anesthetized with pentobarbital (80 mg/kg, i.p.), the right femoral artery and vein were exposed, dissected free, and excised (13). Experimental procedures were performed according to Kyoto University standards for animal care.

Hindlimb blood flow was assessed with a laser Doppler perfusion image (LDPI) analyzer (Moor Instruments, Devon, U.K.) as described (13).

Immunohistochemistry. After fixation with 4% paraformaldehyde, ischemic lower legs were embedded in OCT compound (Sakura Finetechnical, Tokyo) and frozen at −80°C. Cryostat sections (4–8 μm thick) of the tissues were stained with rat anti-mouse platelet EC adhesion molecule-1 (PECAM-1) (PharMingen), mouse anti-α smooth muscle actin (SMA) (Sigma), rat anti-mouse CD45 (PharMingen), rabbit anti-cGKI (Calbiochem), rabbit anti-guanylyl cyclase A (GC-A) and B (GC-B) antibody that we developed (20), rabbit anti-Erk1/2 and phospho-Erk1/2 (Thr-202/Tyr-204) antibody (Cell Signaling Technology, Beverly, MA), or mouse anti-CNP antibody that we developed (KY-CNP-1; ref. 21). As the negative control, rabbit preimmune serum or normal Ig fraction (DAKO) was used to show antibody specificity.

Analysis of Capillary Density and Inflammation. Four random fields on two different sections (≈3 mm apart) from each mouse were photographed with a digital camera (Olympus, Tokyo). By computer-assisted analysis using NIH IMAGE, capillary density was calculated as the mean number of capillaries stained with PECAM-1 (endothelial marker) or α SMA (vascular smooth muscle marker), and the mean number of infiltrating CD45-positive leukocytes was counted as the assessment of inflammation.

Evaluation of *in Situ* Reactive Oxygen Production. The oxidative fluorescent dye dihydroethidium (2×10^{-6} M) was used to evaluate the *in situ* concentration of superoxide in ischemic hindlimb tissue, as described (22). We also stained 4-hydroxy-2-nonenal (4-HNE) (Nippon Oil & Fats, Tokyo), an unsaturated aldehyde that can be formed by the peroxidation of unsaturated fatty acids, such as linoleic and arachidonic acids (23).

Capillary Network Formation Assay. Human umbilical vein ECs (Clonetics, Walkersville, MD) were grown in basic medium (EBM2) (Clonetics) containing growth supplements (EGM2) (Clonetics). They (two to three passages, 4×10^4 cells per well) were seeded at Matrigel-coated Cellware 24-well plates (Becton Dickinson) and incubated for 1 h in 100 μl of EBM2 containing 10% FBS. Serum-free medium (400 μl) containing human ANP, BNP, and CNP (Peptide Institute, Osaka) with or without Rp-8-pCPT-cGMP/PD98059 (Calbiochem) were added. After a 10-h incubation, they were fixed with 10% buffered formalin. Two random fields of view in three or four replicate wells were visualized, and images were captured by using the Olympus digital camera. Network formation was assessed by calculating the total area covered by capillaries in each field of view using NIH IMAGE.

Construction of CNP Plasmid and Its Administration to Ligation Model. The full length of rat CNP cDNA (384 bp) was inserted into the pAC-CMVpLpA vector (4). The plasmid DNA was prepared from cultures of pAC-CMVpLpA-transformed *Escherichia coli* by the EndoFree Plasmid Kit (Qiagen, Valencia, CA). After mouse femoral artery ligation, a local injection of plasmid carrying the CNP cDNA (pAC.CMV/CNP) or none (pAC.CMV) was performed (500 μg per mouse in 200 μl of PBS in 10 injection sites). Plasma CNP level was confirmed by an EIA (Phoenix Pharmaceuticals, St. Joseph, MO).

Statistical Analysis. Results are presented as means ± SEM. The statistical significance of differences in the studies was evaluated by ANOVA. A P value < 0.05 was considered significant.

Results

Ischemia-Induced Angiogenesis Was Accelerated in BNP-Tg Mice. Serial blood flow measurements by LDPI revealed that accelerated limb perfusion improvement was observed for up to 12 days in BNP-Tg mice compared with non-Tg mice (Fig. 1 *a* and *b*). The calculated perfusion ratio of ischemic to nonischemic hindlimb was 0.12 ± 0.02 for BNP-Tg vs. 0.06 ± 0.01 for non-Tg at day 4 ($P = 0.002$), 0.46 ± 0.06 vs. 0.24 ± 0.05 at day 8 ($P = 0.006$), and 0.61 ± 0.07 vs. 0.45 ± 0.04 at day 12 ($P = 0.04$), respectively. After 14 days, restoration of perfusion in BNP-Tg mice was close to non-Tg mice, and no significant difference was seen.

Compatible with the result of blood flow measurement, capillary density in the BNP-Tg group (2,265 ± 62 per mm²) at 10 days was significantly higher than that of the non-Tg group (1,778 ± 74 per mm²; $P < 0.0001$; Fig. 1 *e* and *f*). At day 28, capillary density was equivalent in both groups (Fig. 1 *g* and *h*).

Overexpression of BNP Restored Delayed Angiogenesis Induced by NO Blockade. L-NAME administration to non-Tg mice disclosed impaired recovery in hindlimb perfusion compared with the non-Tg without L-NAME group (Fig. 1*c*). The ratio of ischemic/normal blood flow measured at 14 days was 0.37 ± 0.04 for the non-Tg (+L-NAME) and significantly lower compared with 0.43 ± 0.03 for the non-Tg alone ($P = 0.015$). After 14 days, the ratio of both groups became similar.

In contrast to non-Tg, L-NAME administration had no significant effect on the ratio of blood perfusion in BNP-Tg at any time point (Fig. 1*d*).

On day 10, capillary density of L-NAME-treated non-Tg mice (1,516 ± 62 per mm²) was lower than that of untreated non-Tg mice ($P = 0.014$; Fig. 1 *e* and *f*). In contrast, no difference was seen in BNP-Tg with (2,113 ± 27 per mm²) or without L-NAME administration (day 10). Capillary density in the L-NAME-treated BNP-Tg group was significantly higher than that of the L-NAME-treated non-Tg group ($P = 0.023$) (day 10). On day 28, capillary density was equivalent in these four groups (Fig. 1 *g* and *h*).

Maturity of Newly Formed Blood Vessels in BNP-Tg Mice. From double immunostaining of ischemic hindlimb tissue with PE-CAM-1 and α SMA, the structure of capillaries (ECs with adhering mural cells) showed no apparent difference between BNP-Tg and non-Tg mice (data not shown). Accordingly, immunostaining of the ischemic hindlimb tissues at day 10 with anti-αSMA antibody revealed significantly increased α SMA-positive capillary density in BNP-Tg mice (2,061 ± 65 per mm²) compared with non-Tg mice (1,578 ± 79 per mm²; $P = 0.0001$; Fig. 2 *a* and *b*). In addition, edema or bleeding in the ischemic hindlimb tissues was not observed in BNP-Tg mice.

Focal Inflammation in BNP-Tg Mice. In both BNP-Tg and non-Tg mice, the number of CD45-positive infiltrating leukocytes of the ischemic hindlimb tissues increased until day 5, then gradually decreased (Fig. 2*c*). At day 7, infiltrating leukocytes in BNP-Tg mice were significantly lower than those of non-Tg mice ($P = 0.002$), and no significant difference was seen at days 3, 5, and 10.

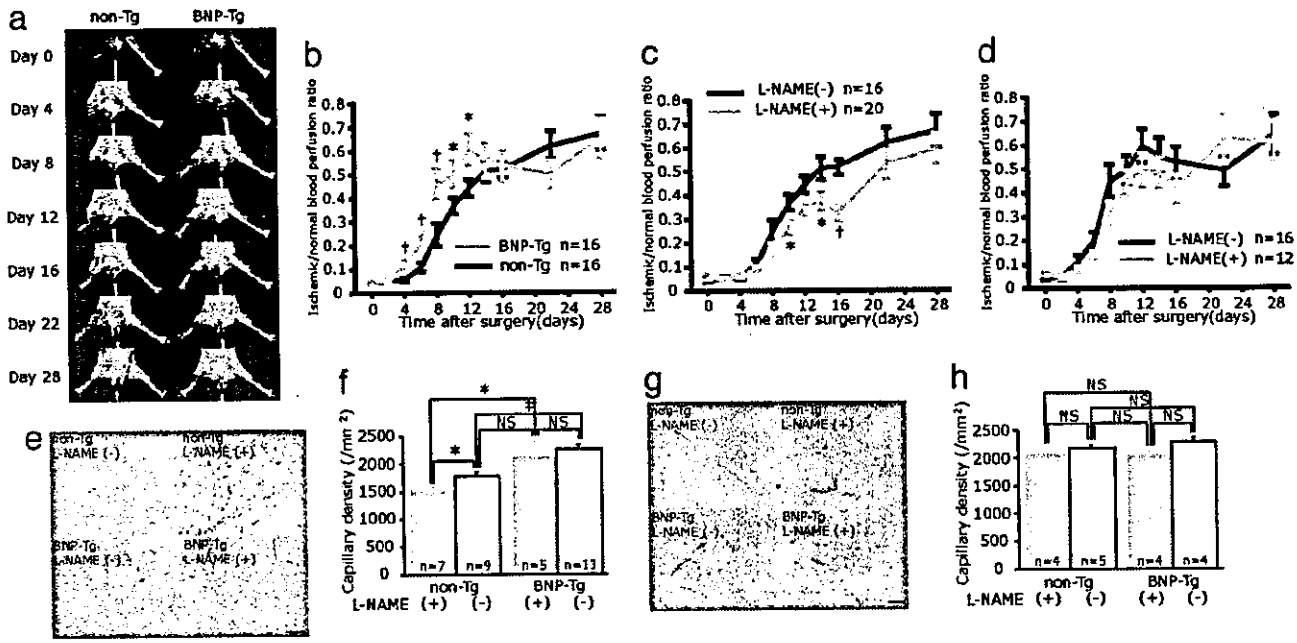

Fig. 1. Ischemia-induced angiogenesis was accelerated in BNP-Tg mice, and overexpression of BNP restored delayed angiogenesis induced by NO blockade. (*a*) Serial LDPI analysis of hindlimb ischemia in BNP-Tg and non-Tg mice. (*b*) Quantitative analysis of ischemic/normal hindlimb perfusion ratio in BNP-Tg and non-Tg mice. (*c* and *d*) Serial LDPI measurements in non-Tg (*c*) and BNP-Tg (*d*) mice with and without L-NAME treatment. (*e* and *g*) Immunostaining of the ischemic hindlimb tissues with anti-PECAM-1 antibody (bright red) at day 10 (e) and day 28 (*g*). (*f* and *h*) Quantitative analysis of capillary density at day 10 (*f*) and day 28 (*h*). *, $P < 0.05$; †, $P < 0.01$; ‡, $P < 0.001$; NS, not significant. (Scale bar, 100 μm.)

Reactive Oxygen Production in Blood Vessels of Ischemic Hindlimb Tissue. By dihydroethidium staining of ischemic hindlimb tissue at day 7, *in situ* concentration of superoxide in the blood vessels of BNP-Tg mice was obviously lower than that of non-Tg mice (Fig. 2*d*). Furthermore, immunostaining of 4-HNE demonstrated that reactive oxygen production was also suppressed in

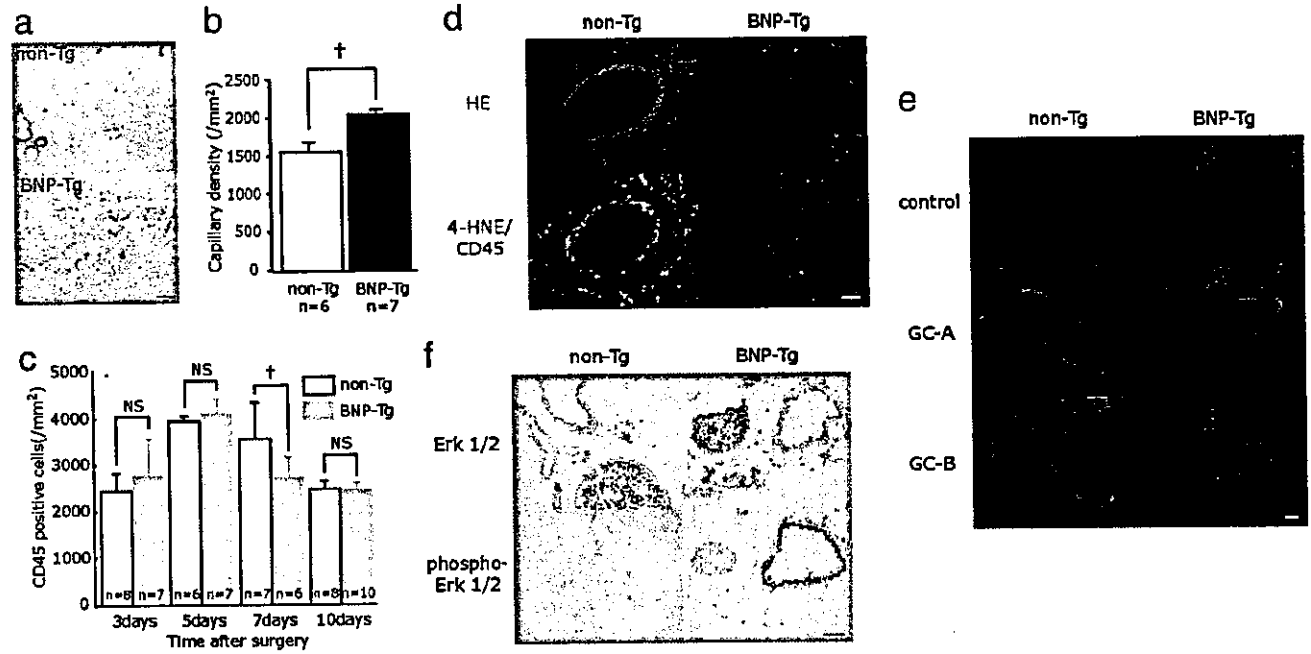

Fig. 2. Evaluation of ischemic hindlimb tissue of BNP-Tg mice. (*a* and *b*) α SMA staining (purple) of the ischemic hindlimb tissues at day 10 (*a*) and quantitative analysis of capillary density (*b*). (*c*) Time course of focal inflammation of ischemic hindlimb obtained from immunostaining with anti-CD45 antibody. (*d*) Dihydroethidium (HE) staining (*Upper*, red) and 4-hydroxy-2-nonenal (4-HNE)/CD45 staining (*Lower*, green fluorescence/red) of the ischemic hindlimb tissue at day 7. (*e*) Expression of GC-A and GC-B (green fluorescence) in the ischemic hindlimb at day 7. Negative controls for these antibodies are also shown. (*f*) Immunostaining of the ischemic hindlimb tissues at day 7 with anti-Erk1/2 or phosphor-Erk1/2 antibody (brown). †, $P < 0.01$. (Scale bars: *a*, 100 μm; *d–f*, 25 μm.)

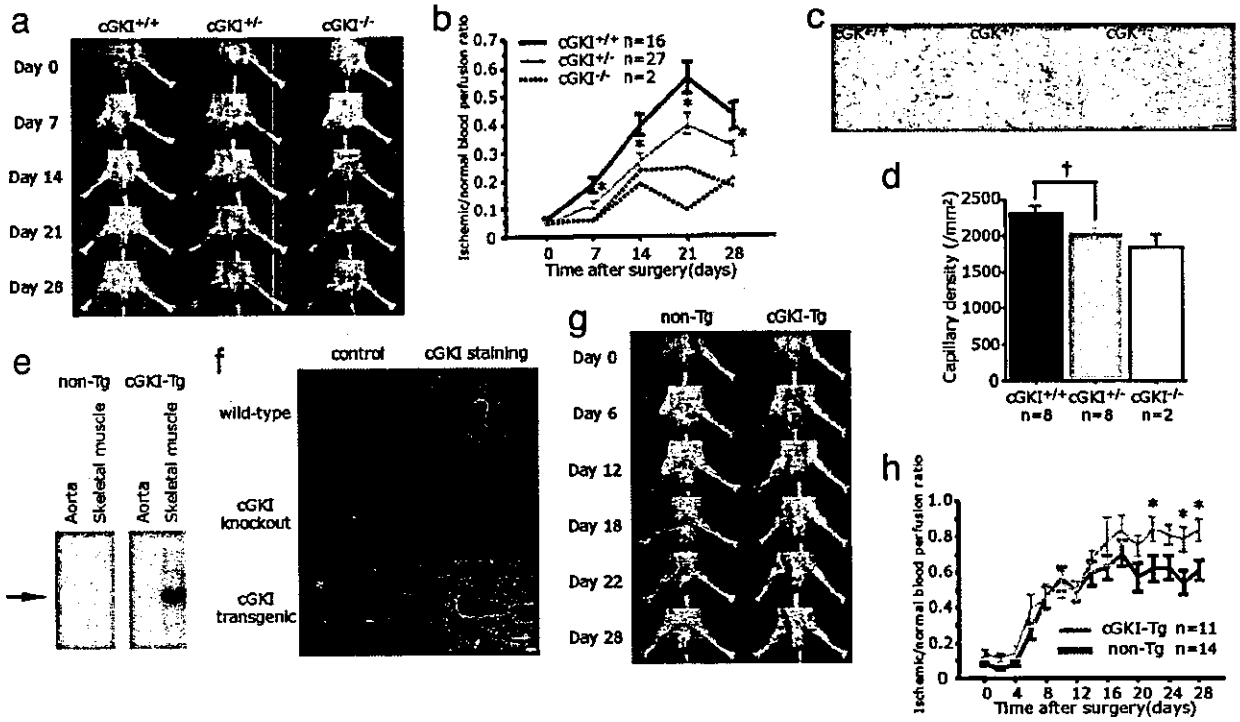

Fig. 3. Angiogenesis was blunted in cGKI-knockout mice and accelerated in cGKI-Tg mice. (*a* and *b*) Serial LDPI measurements in cGKI-knockout mice. (*c* and *d*) PECAM-1 staining (bright red) of the ischemic hindlimb tissues at day 28 in cGKI-Tg mice (*c*) and quantitative analysis of capillary density (*d*). (*e*) The expression of cGKI mRNA in non-Tg and cGKI-Tg mice. (*f*) Immunostaining of cGKI (green fluorescence) with their negative control in WT, cGKI-knockout, and cGKI-Tg mice. (*g* and *h*) Serial LDPI measurements in cGKI-Tg mice. *, $P < 0.05$; †, $P < 0.01$. (Scale bars: *c*, 100 μm; *f*, 25 μm.)

BNP-Tg. From double immunostaining with CD45 in non-Tg mice, reactive oxygen production was prominent in infiltrating leukocytes around and within the blood vessels, as well as SMCs. In BNP-Tg mice, the number of reactive oxygen-positive inflammatory cells was decreased and reactive oxygen production in SMCs was diminished.

Expression of GC-A and GC-B in Ischemic Hindlimb Tissue. Immunostaining (after antigen retrieval) of these receptors in ischemic hindlimb tissue at day 7 revealed that GC-A and GC-B were similarly expressed in the blood vessels of both BNP-Tg and non-Tg mice (Fig. 2*e*). Negative controls showed virtually no significant staining in these serial sections.

Expression of Erk1/2 and Phospho-Erk1/2 in Ischemic Hindlimb Tissue. By immunostaining of Erk1/2 in ischemic hindlimb tissue at day 7, Erk1/2 was equally expressed in ECs and SMCs of both BNP-Tg and non-Tg mice. On the other hand, the expression of phospho-Erk was obviously enhanced in BNP-Tg mice, compared with non-Tg mice (Fig. 2*f*).

Angiogenesis Was Blunted in cGKI-Knockout Mice and Accelerated in cGKI-Tg Mice. The constitution of the homozygous mice gradually deteriorated and most of them died before 10 wk (15). Because nutrition may influence angiogenesis, we mainly compared heterozygous mutant mice ($cGKI^{+/-}$) with their control littermates ($cGK^{+/+}$). By LDPI analysis, limb perfusion among $cGKI^{+/-}$ mice remained significantly impaired throughout the 28-day follow-up period in comparison with $cGK^{+/+}$ (Fig. 3 *a* and *b*). In two cGKI-knockout mice ($cGKI^{-/-}$), recovery from limb ischemia was remarkably reduced, compared with $cGKI^{+/-}$ or $cGK^{+/+}$. Immunostaining of ischemic hindlimb tissue at day 28 with anti-PECAM-1 antibody revealed decreased capillary density in $cGKI^{+/-}$ (2,025 ± 51 per mm^2) compared with $cGK^{+/+}$ (2,302 ± 87 per mm^2; $P = 0.010$; Fig. 3 *c* and *d*). Two $cGKI^{-/-}$ mice had decreased capillary density (1,845 ± 163 per mm^2) compared with $cGKI^{+/-}$ or $cGKI^{+/+}$.

By Northern blotting of cGKI-Tg mice, we confirmed overexpression of cGKI observed in the aorta and skeletal muscle compared with non-Tg mice (Fig. 3*e*). By immunostaining of cGKI, after antigen retrieval, high expression was also seen in the skeletal muscle and blood vessels (Fig. 3*f*). By LDPI analysis, cGKI-Tg mice showed significantly higher perfusion improvement at the end of the study compared with non-Tg mice (Fig. 3 *g* and *h*).

NPs Potentiated Capillary Network Formation of Cultured ECs. NPs significantly potentiated capillary network formation of human umbilical vein ECs in a bell-shaped fashion (Fig. 4 *a* and *b*). Network formation was prominent at 10^{-8} M ANP, 10^{-8} M BNP, and 10^{-10} M to 10^{-8} M CNP. The increase of network formation induced by NPs was completely blocked by Rp-8-pCPT-cGMP, a cGK inhibitor, at a concentration of 5×10^{-6} M (Fig. 4 *a* and *c*). Furthermore, treatment with 10^{-5} M PD 98059, an Erk1/2 inhibitor, significantly suppressed the increase of network formation induced by NPs (Fig. 4 *a* and *d*).

CNP Gene Transfer Enhanced Angiogenesis in Ischemic Hindlimb. CNP immunostaining was detected in skeletal muscle from the ischemic hindlimb of mice that received pAC.CMV/CNP at day 20 (Fig. 5*a*). Endogenous CNP was also detected in blood vessels of mice that received control vector, pAC.CMV (Fig. 5*a*; arrowhead). Plasma CNP level was similarly below sensitivity threshold value ($<1.32 \times 10^{-10}$ M) in mice injected with pAC.CMV/CNP or pAC.CMV. By LDPI analysis, mice receiving pAC.CMV/CNP showed a significant increase in blood flow at

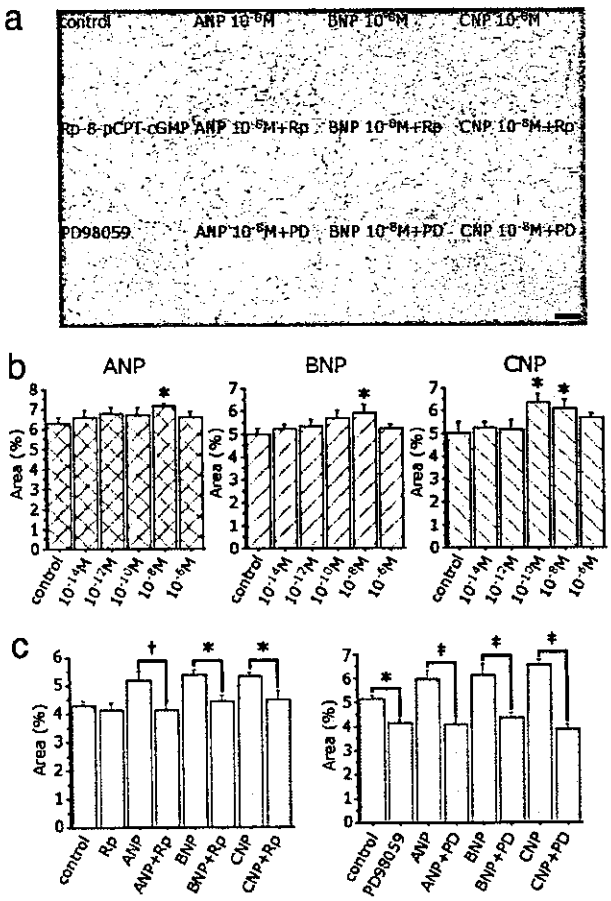

Fig. 4. NPs potentiated capillary network formation of cultured human umbilical vein ECs. (a) Capillary network formation by Matrigel assay in the presence of 10^{-8} M ANP, BNP, and CNP with or without Rp-8-pCPT-cGMP (Rp: 5×10^{-6} M), a cGK inhibitor, and PD 98059 (PD: 10^{-5} M), an Erk1/2 inhibitor. (b) Mean area of tube formation in the presence of various concentrations of ANP, BNP, and CNP. (c and d) Effects of Rp-8-pCPT-cGMP (c) and PD 98059 (d) in network formation induced by NPs. *, $P < 0.05$; †, $P < 0.01$; ‡, $P < 0.001$. (Scale bar, 500 μm.)

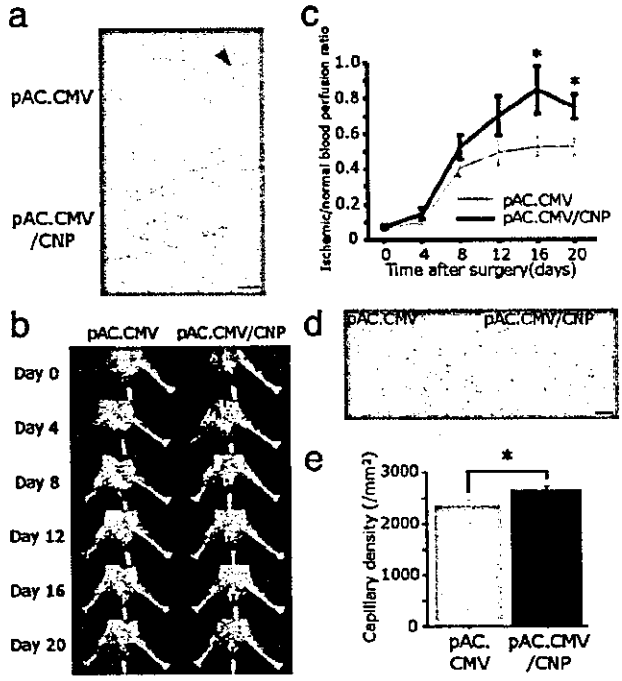

Fig. 5. Effect of CNP gene transfer in the murine ischemic hindlimb model. (a) CNP immunostaining (brown) after local injection of control vector (pAC.CMV) or pAC.CMV/CNP. (b and c) Serial LDPI measurements in mice receiving pAC.CMV or pAC.CMV/CNP ($n = 16$ per group). (d and e) PECAM-1 staining (bright red) of the ischemic hindlimb tissues at day 20 in mice injected with pAC.CMV or pAC.CMV/CNP (d), and quantitative analysis of capillary density (e) ($n = 10$ per group). *, $P < 0.05$. (Scale bars, 100 μm.)

the end of the study compared with mice receiving pAC.CMV (Fig. 5 *b* and *c*). Immunostaining of ischemic hindlimb tissues at day 20 with anti-PECAM-1 antibody revealed an increased capillary density in mice injected with pAC.CMV/CNP (2,643 ± 88 per mm²) compared with pAC.CMV (2,364 ± 104 per mm²; $P = 0.048$; Fig. 5 *d* and *e*).

Discussion

Experiments performed in this study reveal actions of NPs on vascular regeneration in response to ischemia. BNP overproduced systemically in mice accelerated angiogenesis in the setting of tissue ischemia with activation of Erk1/2 in blood vessels. This evidence was confirmed by a combination of LDPI analysis and capillary density measurement. In addition, overproduction of BNP compensated for impaired neovascularization because of L-NAME treatment. We also succeeded in demonstrating that ischemia-induced angiogenesis is significantly potentiated in cGKI-Tg mice, but attenuated in cGK-knockout mice. Furthermore, CNP gene delivery in the ischemic hindlimb could significantly enhance angiogenesis. These results indicate that the NPs/NO/cGMP/cGK pathway is critical for neovascularization *in vivo*.

NPs stimulate two biologically active receptors, GC-A and GC-B. We and others have demonstrated that ANP and BNP show high affinity for GC-A, whereas CNP selectively binds to GC-B (24). We have already reported that BNP-Tg mice show skeletal phenotypes through activation of the CNP/GC-B pathway (16, 24). It is important to clarify, therefore, whether the effects of BNP in the hindlimb ischemia model of BNP-Tg mice are mediated through GC-A, GC-B, or both. By immunostaining of these receptors in the ischemic hindlimb of BNP-Tg mice, we confirmed that both GCs expressed in ECs and SMCs. Considering the finding that CNP also enhanced angiogenesis in our model, activation of GC-B is more likely in BNP-Tg mice; however, the analyses of GC-A-knockout mice (25), which we recently developed, would provide answers to that question.

To supplement these *in vivo* findings with genetically engineered mouse models, we performed several *in vitro* experiments. In cultured ECs, NPs significantly increased capillary network formation at the concentrations of 10^{-10} to 10^{-8} M, which were the same as the plasma BNP level in BNP-Tg mice (14, 16). Early studies, including our own report, have shown that NPs inhibit EC proliferation (26) and migration (27). The concentrations of NPs used in these reports are much higher than physiological (1, 2) and, thus, the EC growth inhibition by NPs seems to be a result of a pharmacological effect. We also confirmed that NP-induced capillary network formation was significantly blocked by Rp-8-pCPT-cGMP and PD98059, indicating the involvement of cGK and Erk1/2 in this phenomenon. Furthermore, we recently observed that ANP increases cultured EC proliferation and migration *in vitro* by activating the cGK and subsequent Akt/PKB and Erk1/2 pathways (28). These results indicate that NPs can act directly on ECs and potentiate endothelial regeneration.

To achieve recovery from tissue ischemia, not only ECs but also SMCs must migrate and proliferate to produce functionally mature vessels (29). Early studies, including our own report, have

shown that NPs inhibit cell growth of vascular SMCs (3). From these reports, it is anticipated that newly formed vessels of BNP-Tg mice in our model might represent immature capillaries without adequate mural cell coating. However, we confirmed that ECs possessed adhering mural cells, and the capillary structures were not different in BNP-Tg or non-Tg mice. Furthermore, the α SMA-positive capillary density in BNP-Tg mice was significantly increased compared with non-Tg mice. These results suggest that antiproliferative effects of NPs on SMCs may not play a role in angiogenesis.

Recently, the participation of inflammation in angiogenesis has been an area of focus. Arras *et al.* (30) reported monocyte activation with the production of cytokines and vessel proliferation might associate with angiogenesis in a rabbit hindlimb ischemia model. Izumi *et al.* (31) reported that infarct size after myocardial ischemia/reperfusion injury was smaller in mice lacking GC-A, accompanied with decreases in neutrophil infiltration. From these results, angiogenesis in our model could be explained in part by potential proinflammatory effects of NPs. However, we confirmed that the number of infiltrating leukocytes in the ischemic limb of BNP-Tg mice was similar or even lower than that of non-Tg mice. This finding indicates that possible proinflammatory effects of NPs do not play a role in angiogenesis.

Nitrates, which are clinically used to relieve coronary vasoconstriction, might be useful for the management of vascular obstructions because NPs and NO share the same intracellular signal-transduction pathway. However, there is growing evidence that nitroglycerin-induced production of oxygen-derived free radicals such as superoxide plays an important role in mediating the tolerance and endothelial dysfunction in response to long-term treatment (32). However, the present study revealed that NPs suppress reactive oxygen production in inflammatory cells and blood vessels. Therefore, our findings suggest that NPs possess clinical advantages over nitrates.

The time course of vascular regeneration was different between BNP-Tg mice and cGKI-Tg/knockout mice. The changes in vascular regeneration in cGKI-Tg and cGKI-knockout mice were clearly opposite ("mirror image") and the continuous activation or inactivation of cGKI might result in the final augmentation or suppression of vascular regeneration, which indicates the significance of the cGKI activation level to determine the extent of vascular regeneration. On the other hand, no significant difference in the blood flow or capillary density was seen between BNP-Tg and non-Tg mice at the end of our study. Attenuation of overactivation of the cGMP/cGKI pathway can be one of the possible explanations; however, the expression of GC-A/GC-B showed no apparent difference between BNP-Tg and non-Tg mice at day 7, and also before ischemia (data not shown). Therefore, even if the attenuation of overactivation of cGKI might be the cause, it must not have occurred at the level of regulation of receptor expression.

Clinical applications of cardiovascular gene therapy have been launched during the last several years. However, we know very little about either the therapeutic or toxic effects of overexpressing angiogenic proteins, including VEGF. VEGF overexpression could accelerate atherosclerosis (33), promote pathological angiogenesis (34), or develop limb-threatening peripheral edema. Less adverse effects, such as edema, are seen in patients treated with ANP (35). We have demonstrated that NPs are the vasculoprotective factor against atherosclerotic lesion (4, 5). Furthermore, in the present study, we confirmed that angiogenesis was enhanced in hindlimb-ischemic mice after CNP gene transfer. From these results, NPs in clinical use seem to possess multiple coordinate actions that result in vascular protection and regeneration. In addition, inhibition of NPs can be a potential target of antineoplastic drugs for suppression of angiogenesis.

In conclusion, we have revealed an activity of the NPs/cGMP/cGKI pathway and suggest that NPs, as endogenous cardiovascular hormones, have significant advantages for the treatment of tissue ischemia. Thus, NPs can be used as a promising strategy for therapeutic angiogenesis in patients with tissue ischemia.

1. Sugawara, A., Nakao, K., Morii, N., Yamada, T., Itoh, H., Shiono, S., Saito, Y., Mukoyama, M., Arai, H., Nishimura, K., *et al.* (1988) *J. Clin. Invest.* **81**, 1962–1970.
2. Mukoyama, M., Nakao, K., Hosoda, K., Suga, S., Saito, Y., Ogawa, Y., Shirakami, G., Jougasaki, M., Obata, K., Yasue, H., *et al.* (1991) *J. Clin. Invest.* **87**, 1402–1412.
3. Komatsu, Y., Itoh, H., Suga, S., Ogawa, Y., Hama, N., Kishimoto, I., Nakagawa, O., Igaki, T., Doi, K., Yoshimasa, T. & Nakao, K. (1996) *Circ. Res.* **78**, 606–614.
4. Doi, K., Ikeda, T., Itoh, H., Ueyama, K., Hosoda, K., Ogawa, Y., Yamashita, J., Chun, T. H., Inoue, M., Masatsugu, K., *et al.* (2001) *Arterioscler. Thromb. Vasc. Biol.* **21**, 930–936.
5. Ohno, N., Itoh, H., Ikeda, T., Ueyama, K., Yamahara, K., Doi, K., Yamashita, J., Inoue, M., Masatsugu, K., Sawada, N., *et al.* (2002) *Circulation* **105**, 1623–1626.
6. Gerber, H. P., McMurtrey, A., Kowalski, J., Yan, M., Keyt, B. A., Dixit, V. & Ferrara, N. (1998) *J. Biol. Chem.* **273**, 30336–30343.
7. Fujio, Y. & Walsh, K. (1999) *J. Biol. Chem.* **274**, 16349–16354.
8. Fulton, D., Gratton, J. P., McCabe, T. J., Fontana, J., Fujio, Y., Walsh, K., Franke, T. F., Papapetropoulos, A. & Sessa, W. C. (1999) *Nature* **399**, 597–601.
9. Dimmeler, S., Fleming, I., Fisslthaler, B., Hermann, C., Busse, R. & Zeiher, A. M. (1999) *Nature* **399**, 601–605.
10. Ziche, M., Morbidelli, L., Choudhuri, R., Zhang, H. T., Donnini, S., Granger, H. J. & Bicknell, R. (1997) *J. Clin. Invest.* **99**, 2625–2634.
11. Hood, J. & Granger, H. J. (1998) *J. Biol. Chem.* **273**, 23504–23508.
12. Parenti, A., Morbidelli, L., Cui, X. L., Douglas, J. G., Hood, J. D., Granger, H. J., Ledda, F. & Ziche, M. (1998) *J. Biol. Chem.* **273**, 4220–4226.
13. Couffinhal, T., Silver, M., Zheng, L. P., Kearney, M., Witzenbichler, B. & Isner, J. M. (1998) *Am. J. Pathol.* **152**, 1667–1679.
14. Ogawa, Y., Itoh, H., Tamura, N., Suga, S., Yoshimasa, T., Uehira, M., Matsuda, S., Shiono, S., Nishimoto, H. & Nakao, K. (1994) *J. Clin. Invest.* **93**, 1911–1921.
15. Pfeifer, A., Klatt, P., Massberg, S., Ny, L., Sausbier, M., Hirneiss, C., Wang, G. X., Korth, M., Aszodi, A., Andersson, K. E., *et al.* (1998) *EMBO J.* **17**, 3045–3051.
16. Suda, M., Ogawa, Y., Tanaka, K., Tamura, N., Yasoda, A., Takigawa, T., Uehira, M., Nishimoto, H., Itoh, H., Saito, Y., *et al.* (1998) *Proc. Natl. Acad. Sci. USA* **95**, 2337–2342.
17. Elhage, R., Bayard, F., Richard, V., Holvoet, P., Duverger, N., Fievet, C. & Arnal, J. F. (1997) *Circulation* **96**, 3048–3052.
18. Tamura, N., Itoh, H., Ogawa, Y., Nakagawa, O., Harada, M., Chun, T. H., Suga, S., Yoshimasa, T. & Nakao, K. (1996) *Hypertension* **27**, 552–557.
19. Niwa, H., Yamamura, K. & Miyazaki, J. (1991) *Gene* **108**, 193–199.
20. Potter, L. R. & Garbers, D. L. (1992) *J. Biol. Chem.* **267**, 14531–14534.
21. Naruko, T., Ueda, M., van der Wal, A. C., van der Loos, C. M., Itoh, H., Nakao, K. & Becker, A. E. (1996) *Circulation* **94**, 3103–3108.
22. Miller, F. J., Jr., Gutterman, D. D., Rios, C. D., Heistad, D. D. & Davidson, B. L. (1998) *Circ. Res.* **82**, 1298–1305.
23. Toyokuni, S., Miyake, N., Hiai, H., Hagiwara, M., Kawakishi, S., Osawa, T. & Uchida, K. (1995) *FEBS Lett.* **359**, 189–191.
24. Chusho, H., Tamura, N., Ogawa, Y., Yasoda, A., Suda, M., Miyazawa, T., Nakamura, K., Nakao, K., Kurihara, T., Komatsu, Y., *et al.* (2001) *Proc. Natl. Acad. Sci. USA* **98**, 4016–4021.
25. Lopez, M. J., Wong, S. K., Kishimoto, I., Dubois, S., Mach, V., Friesen, J., Garbers, D. L. & Beuve, A. (1995) *Nature* **378**, 65–68.
26. Itoh, H., Pratt, R. E., Ohno, M. & Dzau, V. J. (1992) *Hypertension* **19**, 758–761.
27. Ikeda, M., Kohno, M. & Takeda, T. (1995) *Hypertension* **26**, 401–405.
28. Kook, H., Itoh, H., Choi, B. S., Sawada, N., Doi, K., Hwang, T. J., Kim, K. K., Arai, H., Baik, Y. H. & Nakao, K. (2003) *Am. J. Physiol.*, in press.
29. Folkman, J. (1982) *Ann. N.Y. Acad. Sci.* **401**, 212–227.
30. Arras, M., Ito, W. D., Scholz, D., Winkler, B., Schaper, J. & Schaper, W. (1998) *J. Clin. Invest.* **101**, 40–50.
31. Izumi, T., Saito, Y., Kishimoto, I., Harada, M., Kuwahara, K., Hamanaka, I., Takahashi, N., Kawakami, R., Li, Y., Takemura, G., *et al.* (2001) *J. Clin. Invest.* **108**, 203–213.
32. Sage, P. R., de la Lande, I. S., Stafford, I., Bennett, C. L., Phillipov, G., Stubberfield, J. & Horowitz, J. D. (2000) *Circulation* **102**, 2810–2815.
33. Inoue, M., Itoh, H., Ueda, M., Naruko, T., Kojima, A., Komatsu, R., Doi, K., Ogawa, Y., Tamura, N., Takaya, K., *et al.* (1998) *Circulation* **98**, 2108–2116.
34. Tanaka, Y., Katoh, S., Hori, S., Miura, M. & Yamashita, H. (1997) *Lancet* **349**, 1520 (lett.).
35. Saito, Y., Nakao, K., Nishimura, K., Sugawara, A., Okumura, K., Obata, K., Sonoda, R., Ban, T., Yasue, H. & Imura, H. (1987) *Circulation* **76**, 115–124.

Original Article

Adrenomedullin Promotes Proliferation and Migration of Cultured Endothelial Cells

Kazutoshi MIYASHITA, Hiroshi ITOH, Naoki SAWADA, Yasutomo FUKUNAGA, Masakatsu SONE, Kenichi YAMAHARA, Takami YURUGI, and Kazuwa NAKAO

Adrenomedullin (AM) is a vasoactive hormone which exerts its action through cyclic adenosine monophosphate(cAMP) /cAMP-dependent protein kinase (PKA) cascade and intracellular Ca^{2+} mobilization. Recently, evidence has accumulated that AM plays a critical role in the regulation of vascular tone, remodeling and morphogenesis. And although numerous reports have examined the action of AM on cultured vascular cells, the results have not been consistent and have depended on the experimental conditions used. Accordingly, the purpose of this study was to clarify the effect of AM on the proliferation and migration of cultured endothelial cells. Our results revealed that AM promoted the growth and migration of endothelial cells (ECs). AM significantly promoted the proliferation of human umbilical vein endothelial cells (HUVECs) (56.0±8.7% over the controls at 10^{-9} mol/l) and this stimulative effect was inhibited by two AM antagonists, AM(22–52) and calcitonin gene-related peptide (CGRP) (8–37). The number of HUVECs migrated to the lower surface of the transwell apparatus was also increased dose-dependently in the AM group (30.4±4.2% over the controls at 10^{-7} mol/l), and this increase was suppressed by the two AM antagonists and by two PKA antagonists, adenosine 3′,5′-cyclic monophosphorothioate Rp-isomer and myristoylated protein kinase A inhibitor amide 14–22. The promoting action of AM on endothelial migration was also suppressed by LY294002, an inhibitor for phosphatidylinositol 3-kinase, but not by N^{G}-nitro-L-arginine-methyl ester (L-NAME), an antagonist for nitric oxide synthase (NOS). These results indicate that AM promotes proliferation and migration of ECs *via* a cAMP/PKA dependent pathway and lend support to the idea that AM exerts beneficial effects on vascular regeneration and might be used as a novel therapeutic strategy for patients with vascular disease. (*Hypertens Res* 2003; 26 (Suppl): S93–S98)

***Key Words*: adrenomedullin, endothelial cells, proliferation, migration, vascular regeneration**

Introduction

Regeneration of the endothelium after vascular injury is a protective mechanism that limits the development of atherosclerosis (*1*). Postnatal angiogenesis from pre-existing vessels is an important process to alleviate tissue ischemia (*2*). In both processes, proliferation and migration of vascular endothelial cells play critical roles and are regulated by many vasoactive agents.

We have reported the significance of natriuretic peptides (NPs) for the regulation of vascular tone and remodeling. We previously demonstrated that C-type natriuretic peptide (CNP) is secreted from endothelial cells (ECs) to act as a local regulator of vascular tone and growth (*3*). We have also revealed that the endothelial secretion of CNP is stimulated by various cytokines and growth factors that are activated in proliferative vascular lesions and modulate vascular remodeling, especially by transforming growth factor-β and tumor necrosis factor-α (*4*). Furthermore, we revealed that adenovirus-mediated gene transfer of the CNP gene promoted endothelial regeneration accompanied with re-differentiation and

From the Department of Medicine and Clinical Science, Kyoto University Graduate School of Medicine, Kyoto, Japan.
Address for Reprints: Hiroshi Itoh, M.D., Ph.D., Department of Medicine and Clinical Science, Kyoto University Graduate School of Medicine, 54 Shogoin Kawahara-cho, Sakyo-ku, Kyoto 606–8507, Japan. E-mail: hiito@kuhp.kyoto-u.ac.jp
Received August 15, 2002; Accepted in revised form September 17, 2002.

growth suppression of vascular smooth muscle cells (VSMCs) *in vitro* and *in vivo via* an NPs/cyclic guanosine monophosphate (cGMP)/cGMP-dependent kinase (cGK) pathway (*5*, *6*).

Adrenomedullin (AM) is a potent vasorelaxant peptide that was originally isolated from human pheochromocytoma cells on the basis of its ability to elevate cyclic adenosine monophosphate (cAMP) levels in rat platelets (*7*). AM was shown to be secreted from ECs (*8*) and VSMCs (*9*) to act as a local vasorelaxing hormone. AM has also been shown to be present in atherosclerotic lesions, and the AM gene has been identified in macrophages of such lesions (*10*). Its secretion has been augmented by several cytokines, such as interleukin-1, tumor necrosis factor (TNF)-α and lipopolysaccharide (*11*). Furthermore, hypoxia responsive elements (HREs) have been identified in the AM gene, and hypoxic conditions have been shown to induce its expression and secretion from human umbilical vein endothelial cells (HUVECs) (*12*). These findings suggest the significance of AM for atherogenesis and angiogenesis. Recently, mice genetically engineered to overexpress or underexpress the AM gene were developed to determine the *in vivo* significance of AM. Mice overexpressing the AM gene in their vasculature showed reduced blood pressure, and this effect was abolished by administration of N^G-nitro-L-arginine-methyl ester (L-NAME) (*13*), suggesting that AM-induced vasorelaxation was mediated by an nitric oxide (NO)/cGMP dependent pathway. On the other hand, mice lacking the AM gene did not survive the embryonic stage and showed abnormal vascular structure and subcutaneous hemorrhage (*14*). Heterozygote mice with a disrupted AM gene showed an increase in blood pressure. The plasma AM levels are known to be increased in human patients with congestive heart failure (*15*), renal diseases (*16*) and hypertensive disorders (*17–19*). These observations suggested the significance of AM in vascular morphogenesis and regulation of vascular tone *in vivo*.

There have been more than a few reports on the effect of AM on proliferation and migration of several cell types. AM inhibited the proliferation of rat VSMCs cultured in the presence of 5% serum (*20*), and it also inhibited migration of VSMCs stimulated by 5–10% serum, platelet-derived growth factor (PDGF), or angiotensin II through a cAMP-dependent pathway (*21*, *22*). However, in rat quiescent VSMCs, AM promoted cell proliferation independent of the cAMP/cAMP-dependent protein kinase (PKA) pathway (*23*). Thus AM might show dual activities on the growth of cultured VSMCs depending on the experimental conditions.

The effect of AM on proliferation also depends on cell types. For example, AM has been reported to stimulate proliferation of Swiss 3T3 fibroblasts (*24*), human oral keratinocytes (*25*), and certain tumor cell lines (*26*). On the other hand, it inhibited the proliferation of rat mesangial cells (*27*) and cardiac fibroblasts (*28*).

In cultured ECs prepared from rat aorta and incubated in medium containing 0.25% serum, AM was demonstrated to significantly suppress apoptosis without inducing cell proliferation (*29*). In another report, however, it was shown that AM promoted proliferation of HUVECs (*30*). Thus, there is much room for clarification with respect to the effect of AM on the proliferation and migration of ECs.

Based on these findings, the objective of this study was to determine whether AM promotes proliferation and migration of cultured human endothelial cells, and if so, to determine the possible mechanism of these effects.

Methods

Materials

Human AM, AM(22–52), and calcitonin gene-related peptide (8–37) (CGRP(8–37)) were obtained from the Peptide Institute (Osaka, Japan). Adenosine 3′,5′-cyclic monophosphorothioate Rp-isomer (Rp-cAMP) and myristoylated protein kinase A inhibitor amide 14–22 (PKI), both of which are PKA antagonists, and LY294002, which is an inhibitor for phosphatidylinositol 3-kinase (PI3K), were purchased from Calbiochem (San Diego, USA). L-NAME, an antagonist for nitric oxide synthase (NOS), was purchased from Nakalai Tesque (Kyoto, Japan). Hoechst 33342 was purchased from Molecular Probes (Eugene, USA).

Cell Culture

HUVECs (Clonetics, Waltersville, USA) were grown in the basic medium containing 2% fetal bovine serum (FBS) and growth supplements (EGM-2; Clonetics), as previously reported (*31*). Subconfluent cell cultures between passages 4 and 6 were used for each experiment.

Cell Proliferation Assay

The increase of cell number was assessed by modified MTT assay, as previously reported (*32*). After 48 h of incubation in the basic medium containing 0.5 or 2.0% FBS, Cell Count Reagent SF (Nacalai Tesque) was added and the incubation was continued for another 4 h. The reaction was terminated by cooling the cells on ice, and the absorbance at a wavelength of 450 nm was measured to examine the cell number. The real cell number was confirmed to be linearly proportional to the OD_{450} value.

Cell Migration Assay

Migration assays were performed using a transwell apparatus containing a light-opaque membranous insert (6.4 mm diameter, 3 μm pores) designed to absorb fluorescence (FALCON HTS FluoroBlok Multiwell Insert System; Becton Dickinson, Franklin Lakes, USA). Cells pre-labeled with Hoechst 33342, a membrane-permeable nuclear staining fluorescent agent binding to the AT-rich regions of DNA, were added to the upper chamber at a density of 1×10^5 cells/cm^2 and al-

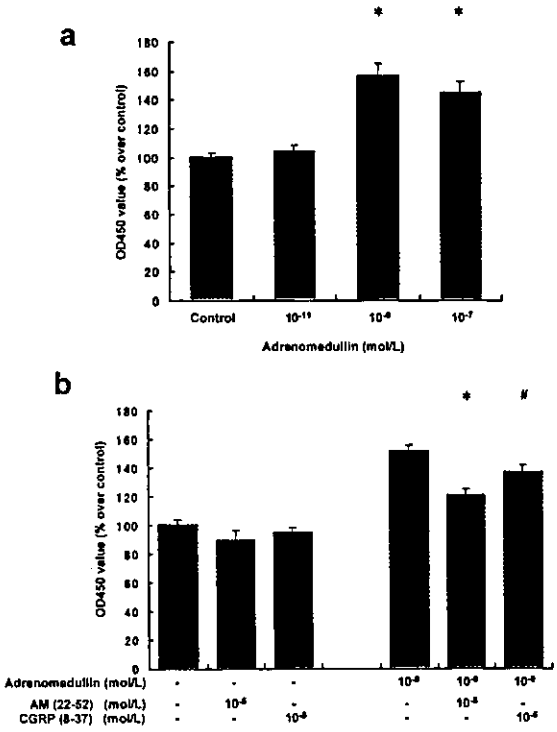

Fig. 1. *AM promoted the proliferation of HUVECs. (a) AM promoted proliferation of HUVECs in medium containing 0.5% serum. The cells were incubated for 48 h and the number of cells was estimated by modified MTT assay.* * $p<0.01$ vs. *controls* ($n=18$). *(b) 10^{-9} mol/l AM-induced proliferation was blocked significantly by two AM antagonists, AM(22–52) (10^{-5} mol/l) and CGRP(8–37) (10^{-5} mol/l).* * $p<0.01$ vs. *controls,* # $p<0.05$ vs. *controls* ($n=18$).

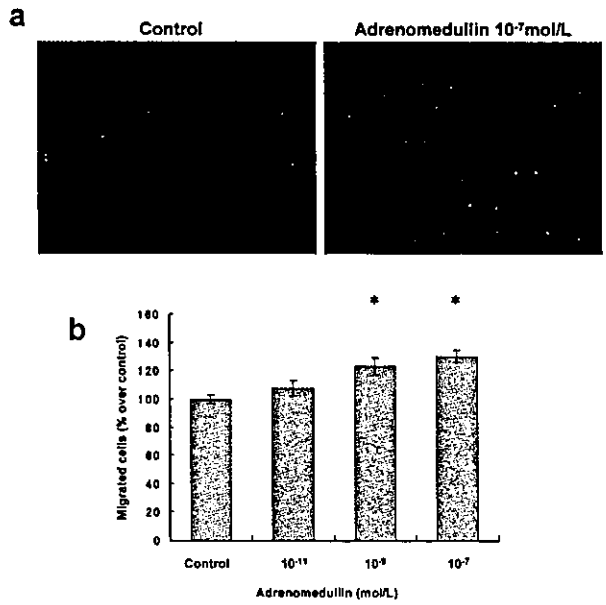

Fig. 2. *AM promoted the migration of HUVECs. (a) The representative images of HUVECs migrated to the lower surface of the transwell apparatus. The cells were pretreated with Hoechst 33342 and allowed to migrate for 4 h. The cells migrated beyond the membranous insert were photographed, and the number of cells was counted with a fluorescent microscope and quantifiable software. (b) AM dose-dependently promoted the migration of HUVECs in the range of 10^{-11}–10^{-7} mol/l. The cells were placed in the upper chamber and AM was added to the lower chamber for chemotaxis. The number of HUVECs migrated to the lower surface of the insert was increased in the AM-treated groups.* * $p<0.01$ vs. *controls* ($n=6$).

lowed to migrate for 4 h at 37°C in the serum-free condition. The number of cells that had migrated through the insert was counted using a fluorescent microscope (Axiovert S100 and AxioCam MRc; Carl Zeiss, Oberkochen, Germany) and software for quantification (Scion Image 0.4.0.2; Scion Corp., Fredevick, USA) (*33*). Four fields (×100 magnification) were photographed for each well. In some experiments, cells were pretreated for 30 min with several inhibitors of the AM/cAMP/PKA pathway to confirm the specificity of the migratory effect of AM.

Statistics

All data are expressed as the mean±SEM. Statistical analysis was performed with Student's *t* test or analysis of variance (ANOVA). Values of $p<0.05$ were considered to indicate statistical significance.

Results

AM Promoted Proliferation of the Cultured Endothelium

AM dose-dependently increased the number of HUVECs incubated for 48 h in the medium containing 0.5% FBS (Fig. 1a). The proliferative effect of 10^{-9} mol/l AM was 56.0± 8.7% over the control value ($p<0.01$ *vs.* controls), and no further increase in cell number was observed at a concentration of 10^{-7} mol/l AM. The proliferative effect of AM on ECs was reduced by the higher concentration (2.0%) of FBS (11.9±3.3% over the control value at 10^{-11} mol/l, $p<0.05$; 13.9±2.9% at 10^{-9} mol/l, $p<0.05$; 13.0±2.8% at 10^{-7} mol/l, $p<0.05$ *vs.* controls: $n=6$ in each group) AM-induced proliferation was blocked significantly with two AM antagonists, AM(22–52) (10^{-5} mol/l) and CGRP(8–37) (10^{-5} mol/l), when ECs were stimulated by 10^{-9} mol/l AM in 0.5% serum (Fig. 1b).

AM Promoted Migration of the Cultured Endothelium

Figure 2a shows the effect of 10^{-7} mol/l AM on the migration of cultured HUVECs compared with the control value. As shown in the photographs, the number of HUVECs migrated to the lower surface of the insert was increased in the AM-treated group. Figure 2b demonstrates the dose-dependent effect of AM on the migration of HUVECs.

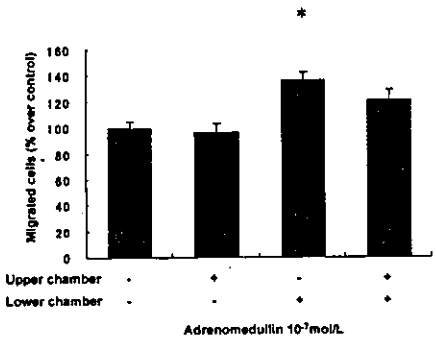

Fig. 3. *AM-induced migration was chemotactic. AM (10^{-7} mol/l) was added to either the upper, lower or both chambers. The number of migrated cells was significantly increased in the group in which AM was added to the lower chamber only.* * $p<0.01$ vs. *controls (the group without AM)* ($n=6$).

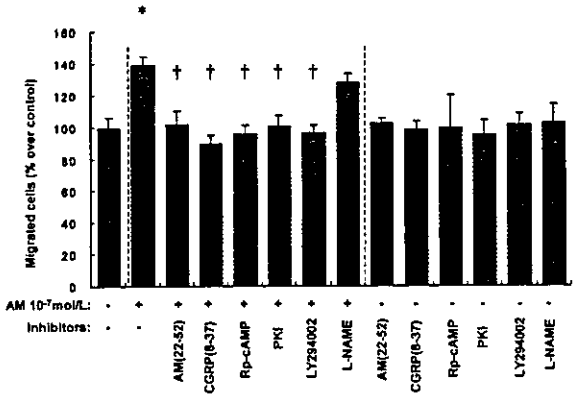

Fig. 4. *AM-induced migration was inhibited by blockade of the AM/cAMP/PKA cascade. AM-induced migration was blocked significantly by pretreatment with AM(22–52) (10^{-5} mol/l) or CGRP(8–37) (10^{-5} mol/l), and with Rp-cAMP (5×10^{-6} mol/l) or PKI (5×10^{-6} mol/l). It was also suppressed with LY294002 (2×10^{-5} mol/l). However, L-NAME (10^{-5} mol/l) did not significantly affect the AM-induced migration.* * $p<0.01$ vs. *controls (the group in which neither AM nor inhibitor was added),* † $p<0.01$ vs. *AM alone (the group in which AM (10^{-7} mol/l) was added in the lower chamber without inhibitors)* ($n=6$).

AM Promoted Migration of the Endothelium in a Chemotactic Manner

The migratory process contains two components: chemotaxis and chemokinesis. We therefore evaluated whether AM exerts a chemotactic or chemokinetic influence (or both) on ECs. The chemotactic property was determined by the migratory effect of AM (10^{-7} mol/l) when it was added to the lower chamber only, and the chemokinetic property was determined by adding AM to both the lower and upper chambers. As shown in Fig. 3, AM significantly promoted endothelial migration when it was added to the lower chamber only. This result indicates that AM-induced migration was chemotactic for cultured HUVECs.

AM-Induced Migration Was Mediated by the cAMP/PKA Pathway

As shown in Fig. 4, AM (10^{-7} mol/l in the lower chamber)-induced migration was blocked significantly by pretreatment with the two AM antagonists, AM(22–52) (10^{-5} mol/l) and CGRP(8–37) (10^{-5} mol/l). The migratory response induced by AM was also significantly suppressed by the PKA inhibitors, Rp-cAMP (5×10^{-6} mol/l) and PKI (5×10^{-6} mol/l). In addition, the inhibitor of PI3K, LY294002 (2×10^{-5} mol/l), significantly suppressed AM-induced migration of EC, but in contrast, L-NAME (10^{-5} mol/l) had no significant effect. The inhibitors at the doses used in the present study had no apparent effect on basal endothelial migration in the serum-free medium.

Discussion

In this study, we demonstrated that the proliferation and migration of HUVECs were augmented by AM in a dose-dependent manner, and that the AM antagonists (AM(22–52), CGRP(8–37)) blocked these effects. The AM-induced migration was predominantly chemotactic and was inhibited by the PKA antagonists (Rp-cAMP, PKI) and also the PI3K inhibitor (LY294002), but was not inhibited by the NOS antagonist (L-NAME).

In previous reports, the effect of AM on proliferation and migration varied according to the cell types and experimental conditions used. The dependency on the cAMP/PKA pathway of AM-induced biological effects on vascular cells was also different in each report. AM exerted an anti-proliferative effect on VSMCs explanted from rat aorta and incubated in medium with 5% serum (*20*). In this report, the inhibitory process was thought to be cAMP-dependent. AM was also reported to inhibit proliferation of rat glomerular mesangial cells (*27*) and rat cardiac fibroblasts (*28*) in a cAMP/PKA-dependent manner. On the other hand, in quiescent VSMCs prepared from rat aorta and made quiescent by incubation with serum-free medium for 2–3 days, AM was shown to stimulate DNA synthesis and cell proliferation with an increase in mitogen-activated protein kinase (MAP kinase) activity (*23*). In this case, the proliferative process was thought to be independent of the cAMP/PKA pathway. Furthermore, AM receptor antagonism with CGRP(8–37) inhibited rat carotid artery neointimal hyperplasia (*34*), which implies the significance of endogenous AM in balloon injury-induced proliferation of VSMCs, although the anti-proliferative effect could be caused by the blockade of the CGRP activity because CGRP(8–37) might antagonize both AM and CGRP receptors. With regard to migration of cultured VSMCs, it has been reported that AM inhibited the migration of VSMCs stimulated by 5–10% serum, PDGF, or

angiotensin II (*21*, *22*), and the inhibitory process was thought to be dependent on the cAMP/PKA pathway.

In the case of the vascular endothelium, reports have shown that AM had an anti-apoptotic effect on ECs incubated in 0.25% serum or in the absence of serum, and that this effect appeared to be mediated by a mechanism not related to the cAMP/PKA pathway (*29*, *35*). In this report, AM neither induced cell proliferation nor stimulated [^{3}H]thymidine incorporation of rat ECs in medium containing 0.25% serum (*29*). In another report, however, it was shown that AM promoted the proliferation of HUVECs cultured in medium containing 10% serum (*30*). With regard to the effect of AM on migration of ECs, there has been no previous report as far as we know.

In this study, we revealed that AM promoted the proliferation and migration of HUVECs incubated in medium with 0.5–2.0% serum and in the absence of serum, respectively. Furthermore, the migratory effect appeared to be dependent on the cAMP/PKA cascade. We previously reported that AM increased cAMP production and exerted an antiproliferative action on bovine aortic endothelial cells (BAECs) (*36*). In that report, we showed that exogenously administered AM inhibited PDGF-stimulated DNA synthesis in a dose-dependent manner and that neutralization of endogenously secreted AM by the monoclonal antibody against AM increased [^{3}H]thymidine uptake. The experimental conditions of that study differed from those of the present study in several points: the former study employed a higher concentration of serum, showed a potent stimulation of cellular proliferation by PDGF, and employed endothelial cells from different animal species (BAECs). Together with previous reports, these results lead us to assume that one of the critical factors which determine the effect of AM on proliferation of VSMCs and ECs is the serum concentration used in the experiments. In the present study, we tried to determine the effects of different serum concentrations (0.5% and 2.0%) on AM-induced proliferation, and we found that the higher concentration of serum (2.0%) reduced the proliferative effect of AM on ECs.

Recently, there has been accumulating evidence that the NO and NPs/cGMP/cGK pathways are significant for regulation of not only vascular tone but also vascular remodeling and postnatal angiogenesis (*37*). NO is also known to mediate vascular endothelial growth factor (VEGF)-induced proliferation of ECs and angiogenesis (*38*) by activating the cGMP/cGK pathway. As for AM-induced vasodilatation, it has already been reported that activation of the NO/cGMP pathway plays a significant role (*39*). However, it remains to be clarified how significant this pathway is for AM-induced cell proliferation and migration of VSMCs and ECs. It was previously shown that the anti-apoptotic effect of AM was mediated by NO, but this effect of NO was thought to be independent of the cGMP/cGK pathway (*35*). In this study, we tried to examine the involvement of NO in the migratory effect of AM on ECs. The administration of L-NAME, however, had no significant effect on the AM-induced migration. This result suggests that AM-induced migration is not mediated by the NO pathway.

Recent studies support the significance of the PI3K/Akt pathway in endothelial regeneration and postnatal angiogenesis (*40*). Furthermore, it has been shown that AM promoted Akt phosphorylation of rat aorta in a time- and dose-dependent manner and induced NO production and vasodilation (*41*). Accordingly, we here examined the involvement of the PI3K/Akt pathway in AM-induced migration of ECs. The PI3K inhibitor, LY294002, significantly suppressed AM-induced migration, which suggests involvement of the PI3K/Akt pathway in AM-induced migration of ECs. We have also confirmed the augmentation of Akt phosphorylation by administration of AM to HUVECs (data not shown). We are further investigating the relationship and molecular mechanism of Akt phosphorylation and cell migration induced by AM.

In summary, we revealed that the AM/cAMP/PKA cascade promotes the proliferation and migration of the cultured endothelium. Thus the AM/cAMP/PKA cascade or its downstream molecules might be useful as a therapeutic target to modulate vascular remodeling or support vascular regeneration.

References

1. Ross R: The pathogenesis of atherosclerosis: a perspective for the 1990s. *Nature* 1993; **362**: 801–809.
2. Carmeliet P: Mechanisms of angiogenesis and arteriogenesis. *Nat Med* 2000; **6**: 389–395.
3. Komatsu Y, Itoh H, Suga S, *et al*: Regulation of endothelial production of C-type natriuretic peptide in coculture with vascular smooth muscle cells: role of the vascular natriuretic peptide system in vascular growth inhibition. *Circ Res* 1996; **78**: 606–614.
4. Suga S, Nakao K, Itoh H, *et al*: Endothelial production of C-type natriuretic peptide and its marked augmentation by transforming growth factor-β; possible existence of vascular natriuretic peptide system. *J Clin Invest* 1992; **90**: 1145–1149.
5. Doi K, Ikeda T, Itoh H, *et al*: C-type natriuretic peptide induces redifferentiation of vascular smooth muscle cells with accelerated reendothelialization. *Arterioscler Thromb Vasc Biol* 2001; **21**: 930–936.
6. Ohno N, Itoh H, Ikeda T, *et al*: Accelerated reendothelialization with suppressed thrombogenic property and neointimal hyperplasia of rabbit jugular vein grafts by adenovirus-mediated gene transfer of C-type natriuretic peptide. *Circulation* 2002; **105**: 1623–1626.
7. Kitamura K, Kangawa K, Kawamoto M, *et al*: Adrenomedullin: a novel hypotensive peptide isolated from human pheochromocytoma. *Biochem Biophys Res Commun* 1993; **192**: 553–560.
8. Sugo S, Minamino N, Kangawa K, *et al*: Endothelial cells actively synthesize and secrete adrenomedullin. *Biochem Biophys Res Commun* 1994; **201**: 1160–1166.
9. Sugo S, Minamino N, Shoji H, *et al*: Production and secretion of adrenomedullin from vascular smooth muscle cells: augmented production by tumor necrosis factor-α. *Biochem*

Biophys Res Commun 1994; **203**: 719–726.
10. Nakayama M, Takahashi K, Murakami O, *et al*: Adrenomedullin in monocytes and macrophages: possible involvement of macrophage-derived adrenomedullin in atherogenesis. *Clin Sci (Lond)* 1999; **97**: 247–251.
11. Sugo S, Minamino N, Shoji H, *et al*: Interleukin-1, tumor necrosis factor and lipopolysaccharide additively stimulate production of adrenomedullin in vascular smooth muscle cells. *Biochem Biophys Res Commun* 1995; **207**: 25–32.
12. Ogita T, Hashimoto E, Yamasaki M, *et al*: Hypoxic induction of adrenomedullin in cultured human umbilical vein endothelial cells. *J Hypertens* 2001; **19**: 603–608.
13. Shindo T, Kurihara H, Maemura K, *et al*: Hypotension and resistance to lipopolysaccharide-induced shock in transgenic mice overexpressing adrenomedullin in their vasculature. *Circulation* 2000; **101**: 2309–2316.
14. Shindo T, Kurihara Y, Nishimatsu H, *et al*: Vascular abnormalities and elevated blood pressure in mice lacking adrenomedullin gene. *Circulation* 2001; **104**: 1964–1971.
15. Jougasaki M, Wei CM, McKinley LJ, Burnett JC Jr: Elevation of circulating and ventricular adrenomedullin in human congestive heart failure. *Circulation* 1995; **92**: 286–289.
16. Ishimitsu T, Nishikimi T, Saito Y, *et al*: Plasma levels of adrenomedullin, a newly identified hypotensive peptide, in patients with hypertension and renal failure. *J Clin Invest* 1994; **94**: 2158–2161.
17. Kato J, Kitamura K, Matsui E, *et al*: Plasma adrenomedullin and natriuretic peptides in patients with essential or malignant hypertension. *Hypertens Res* 1999; **22**: 61–65.
18. Shimosawa T, Kanozawa K, Nagasawa R, *et al*: Adrenomedullin amidation enzyme activities in hypertensive patients. *Hypertens Res* 2000; **23**: 167–171.
19. Nishikimi T, Matsuoka H, Ishikawa K, *et al*: Antihypertensive therapy reduces increased plasma levels of adrenomedullin and brain natriuretic peptide concomitant with regression of left ventricular hypertrophy in a patient with malignant hypertension. *Hypertens Res* 1996; **19**: 97–101.
20. Kano H, Kohno M, Yasunari K, *et al*: Adrenomedullin as a novel antiproliferative factor of vascular smooth muscle cells. *J Hypertens* 1996; **14**: 209–213.
21. Horio T, Kohno M, Kano H, *et al*: Adrenomedullin as a novel antimigration factor of vascular smooth muscle cells. *Circ Res* 1995; **77**: 660–664.
22. Kohno M, Yokokawa K, Kano H, *et al*: Adrenomedullin is a potent inhibitor of angiotensin II–induced migration of human coronary artery smooth muscle cells. *Hypertension* 1997; **29**: 1309–1313.
23. Iwasaki H, Eguchi S, Shichiri M, Marumo F, Hirata Y: Adrenomedullin as a novel growth-promoting factor for cultured vascular smooth muscle cells: role of tyrosine kinase-mediated mitogen-activated protein kinase activation. *Endocrinology* 1998; **139**: 3432–3441.
24. Withers DJ, Coppock HA, Seufferlein T, Smith DM, Bloom SR, Rozengurt E: Adrenomedullin stimulates DNA synthesis and cell proliferation *via* elevation of cAMP in Swiss 3T3 cells. *FEBS Lett* 1996; **378**: 83–87.
25. Kapas S, Brown DW, Farthing PM, Hagi-Pavli E: Adrenomedullin has mitogenic effects on human oral keratinocytes: involvement of cyclic AMP. *FEBS Lett* 1997; **418**: 287–290.
26. Miller MJ, Martinez A, Unsworth EJ, *et al*: Adrenomedullin expression in human tumor cell lines: its potential role as an autocrine growth factor. *J Biol Chem* 1996; **271**: 23345–23351.
27. Chini EN, Choi E, Grande JP, Burnett JC, Dousa TP: Adrenomedullin suppresses mitogenesis in rat mesangial cells *via* cAMP pathway. *Biochem Biophys Res Commun* 1995; **215**: 868–873.
28. Tsuruda T, Kato J, Kitamura K, *et al*: An autocrine or a paracrine role of adrenomedullin in modulating cardiac fibroblast growth. *Cardiovasc Res* 1999; **43**: 958–967.
29. Kato H, Shichiri M, Marumo F, Hirata Y: Adrenomedullin as an autocrine/paracrine apoptosis survival factor for rat endothelial cells. *Endocrinology* 1997; **138**: 2615–2620.
30. Zhao Y, Hague S, Manek S, Zhang L, Bicknell R, Rees MC: PCR display identifies tamoxifen induction of the novel angiogenic factor adrenomedullin by a non estrogenic mechanism in the human endometrium. *Oncogene* 1998; **16**: 409–415.
31. Saito T, Itoh H, Chun TH, *et al*: Coordinate regulation of endothelin and adrenomedullin secretion by oxidative stress in endothelial cells. *Am J Physiol Heart Circ Physiol* 2001; **281**: H1364–H1371.
32. Fukunaga Y, Itoh H, Doi K, *et al*: Thiazolidinediones, peroxisome proliferator-activated receptor γ agonists, regulate endothelial cell growth and secretion of vasoactive peptides. *Atherosclerosis* 2001; **158**: 113–119.
33. Morales DE, McGowan KA, Grant DS, *et al*: Estrogen promotes angiogenic activity in human umbilical vein endothelial cells *in vitro* and in a murine model. *Circulation* 1995; **91**: 755–763.
34. Shimizu K, Tanaka H, Sunamori M, Marumo F, Shichiri M: Adrenomedullin receptor antagonism by calcitonin gene-related peptide(8–37) inhibits carotid artery neointimal hyperplasia after balloon injury. *Circ Res* 1999; **85**: 1199–1205.
35. Sata M, Kakoki M, Nagata D, *et al*: Adrenomedullin and nitric oxide inhibit human endothelial cell apoptosis *via* a cyclic GMP-independent mechanism. *Hypertension* 2000; **36**: 83–88.
36. Michibata H, Mukoyama M, Tanaka I, *et al*: Autocrine/paracrine role of adrenomedullin in cultured endothelial and mesangial cells. *Kidney Int* 1998; **53**: 979–985.
37. Murohara T, Asahara T, Silver M, *et al*: Nitric oxide synthase modulates angiogenesis in response to tissue ischemia. *J Clin Invest* 1998; **101**: 2567–2578.
38. Ziche M, Morbidelli L, Masini E, *et al*: Nitric oxide mediates angiogenesis *in vivo* and endothelial cell growth and migration *in vitro* promoted by substance P. *J Clin Invest* 1994; **94**: 2036–2044.
39. Hayakawa H, Hirata Y, Kakoki M, *et al*: Role of nitric oxide-cGMP pathway in adrenomedullin-induced vasodilation in the rat. *Hypertension* 1999; **33**: 689–693.
40. Kureishi Y, Luo Z, Shiojima I, *et al*: The HMG-CoA reductase inhibitor simvastatin activates the protein kinase Akt and promotes angiogenesis in normocholesterolemic animals. *Nat Med* 2000; **6**: 1004–1010.
41. Nishimatsu H, Suzuki E, Nagata D, *et al*: Adrenomedullin induces endothelium-dependent vasorelaxation *via* the phosphatidylinositol 3-kinase/Akt-dependent pathway in rat aorta. *Circ Res* 2001; **89**: 63–70.

Different Differentiation Kinetics of Vascular Progenitor Cells in Primate and Mouse Embryonic Stem Cells

Masakatsu Sone, MD; Hiroshi Itoh, MD, PhD; Jun Yamashita, MD, PhD; Takami Yurugi-Kobayashi, MD; Yutaka Suzuki, PhD; Yasushi Kondo, PhD; Akane Nonoguchi; Naoki Sawada, MD, PhD; Kenichi Yamahara, MD; Kazutoshi Miyashita, MD; Kwijun Park, MD; Masabumi Shibuya, MD, PhD; Shinji Nito, PhD; Shin-Ichi Nishikawa, MD, PhD; Kazuwa Nakao, MD, PhD

Background—We demonstrated that vascular endothelial growth factor receptor 2 (VEGF-R2)-positive cells derived from mouse embryonic stem (ES) cells can differentiate into both endothelial cells and mural cells to suffice as vascular progenitor cells (VPCs). Here we examined whether VPCs occur in primate ES cells and investigated the differences in VPC differentiation kinetics between primate and mouse ES cells.

Methods and Results—In contrast to mouse ES cells, undifferentiated monkey ES cells expressed VEGF-R2. By culturing these undifferentiated ES cells for 4 days on OP9 feeder layer, VEGF-R2 expression disappeared, and then reappeared after 8 days of differentiation. We then isolated these VEGF-R2–positive and vascular endothelial cadherin (VEcadherin)-negative cells by flow cytometry sorting. Additional 5-day reculture of these VEGF-R2$^+$ VEcadherin$^-$ cells on OP9 feeder layer resulted in the appearance of platelet endothelial cell adhesion molecule-1 (PECAM1)-positive, VEcadherin-positive, endothelial nitric oxide synthase (eNOS)-positive endothelial cells. On a collagen IV-coated dish in the presence of serum, these cells differentiated into smooth muscle actin (SMA)-positive and calponin-positive mural cells (pericytes or vascular smooth muscle cells). Addition of 50ng/mL VEGF to the culture on a collagen IV-coated dish resulted in the appearance of PECAM1$^+$ cells surrounded by SMA$^+$ cells. In addition, these differentiated VEGF-R2$^+$ cells can form tube-like structures in a 3-dimensional culture.

Conclusion—Our findings indicate that differentiation kinetics of VPCs derived from primate and mouse ES cells were different. Differentiated VEGF-R2$^+$ VEcadherin$^-$ cells can act as VPCs in primates. To seek the clinical potential of VPCs for vascular regeneration, investigations of primate ES cells are indispensable. **(*Circulation*. 2003;107:2085-2088.)**

Key Words: angiogenesis ■ cells ■ endothelium ■ muscle, smooth ■ vessels

Embryonic stem (ES) cells with pluripotency and self-renewal are now highlighted as promising cell sources for regeneration medicine. Previously we demonstrated that mouse ES cell-derived vascular endothelial growth factor receptor-2 (VEGF-R2)-positive cells can differentiate into both endothelial cells and mural cells (pericytes and vascular smooth muscle cells) and reproduce the vascular organization process.[1] Vascular cells derived from VEGF-R2$^+$ cells can organize vessel-like structures in a 3-dimensional culture. Mouse ES cell-derived VEGF-R2$^+$ cells can, thus, serve as vascular progenitor cells (VPCs). Furthermore, we have reported that implantation of mouse ES-derived vascular cells into nude mice significantly augmented blood flow in an adult neoangiogenesis model, which suggests the usefulness of ES cell-derived VPCs for vascular regeneration medicine.[2]

Recently primate embryonic stem cell lines were established from blastocysts of both humans and monkeys.[3–6] Primate ES cells possess a number of characteristics distinct from mouse ES cells, such as surface antigens, leukemia inhibitory factor (LIF)-independence, and long doubling times.[3–7] Recent study showed that VEGF-R2 was expressed in undifferentiated human ES cells, unlike in mouse ES cells,[8,9] and continuously expressed during differentiation in embryoid body (EB) formation. It has also been demonstrated that platelet endothelial cell adhesion molecule-1 (PECAM1)-positive cells can be isolated from human EBs,

Received December 31, 2002; revision received March 12, 2003; accepted March 13, 2003.

From the Department of Medicine and Clinical Science (M.S., H.I., T.Y.-K., A.N., N.S., K.Y., K.M., K.P., K.N.) and the Department of Molecular Genetics (J.Y., S.-I.N.), Kyoto University Graduate School of Medicine, Kyoto; the Discovery Research Laboratory, Tanabe Seiyaku Co, Ltd, Osaka (Y.S., Y.K., S.N.); the Department of Genetics, Institute of Medical Science, University of Tokyo, Tokyo (M.S.); and the Center for Developmental Biology, RIKEN, Kobe (S.-I.N.), Japan.

Correspondence to Hiroshi Itoh, MD, PhD, Department of Medicine and Clinical Science, Kyoto University Graduate School of Medicine, 54 Shogoin Kawahara-cho, Sakyo-ku, Kyoto 606-8507 Japan. E-mail hiito@kuhp.kyoto-u.ac.jp

Circulation is available at http://www.circulationaha.org

DOI: 10.1161/01.CIR.0000070022.78747.1B

and they can act as endothelial cells.[9] However, the vascular differentiation process of primate cells has not been demonstrated, and VPCs that can differentiate into both endothelial cells and mural cells have not been characterized in the primates. To elucidate the vascular differentiation process of primate cells and to seek the clinical potential of VPCs for vascular regeneration therapy with the use of an in vitro 2-dimensional differentiation system of ES cells that we established,[10,11] we examined whether and how VPCs occur in primate ES cells in comparison to mouse ES cells.

Methods

Cell Culture

Cynomolgus monkey ES cell lines were established, and their pluripotency was confirmed by teratoma formation in severe combined immunodeficiency mice, as described previously.[6,12] Undifferentiated ES cells were maintained as described.[6,12] OP9 feeder cell lines that were established from mouse calvaria were maintained as described previously.[11,13,14]

To induce differentiation, undifferentiated ES cells were cultured on OP9 feeder layer in differentiation medium (minimal essential medium [GIBCO] supplemented with 10% fetal calf serum (FCS) and 5×10^{-5} M2-mercaptoethanol).[11] Sorted VEGF-R2$^+$ cells were re-cultured on an OP9 feeder layer or collagen IV-coated dish with differentiation medium. Three-dimensional culture was performed as described.[1]

Flow Cytometry and Cell Sorting

At different time points during the differentiation process, cultured cells were harvested by cell dissociation buffer (GIBCO). Flow cytometry analysis and cell sorting were as discribed.[10,11] Monoclonal antibody for VEGF-R2, which we developed,[15] was labeled with Alexa-647 in our laboratory (monoclonal antibody labeling kit, molecular probes). PE-conjugated vascular endothelial cadherin (VEcadherin) antibody and fluorescein isothiocyanate-conjugated PECAM1 antibody were purchased from BD Biosciences. To test the differentiation potential of VEGF-R2$^+$ cells, sorted cells were plated into a collagen IV-coated 96-well dish at the density of 2.5×10^3 cells per well, or plated on OP9 feeder layer in a 24-well dish at 1×10^4 cells per well.

Immunohistochemistry

Staining of culture cells on dishes was as described.[1,11] Monoclonal antibody for smooth muscle actin (SMA) was purchased from Sigma, those for calponin and smooth muscle myosin heavy chain (SMMHC) were purchased from DAKO, and those for PECAM1, VEcadherin, and endothelial nitric oxide synthase (eNOS) were purchased from BD Biosciences.

Results

Although undifferentiated mouse ES cells did not express VEGF-R2, most of undifferentiated monkey ES cells were positive for VEGF-R2 (data not shown). Mouse ES cells differentiated into VEGF-R2$^+$ cells during a 4-day differentiation on OP9 feeder layer. These mouse VEGF-R2$^+$ cells differentiated into endothelial cells during 4 days of re-culturing on a collagen IV-coated dish or OP9 feeder layer.[1,11] In contrast, however, we could not induce endothelial cells from VEGF-R2$^+$ undifferentiated monkey ES cells in the same condition (data not shown). Thus, we examined VEGF-R2 expression on monkey ES cells during differentiation.

Undifferentiated monkey ES cells were dissociated to single cells and plated on an OP9 feeder layer to induce differentiation (Figure 1A). As shown in Figure 1B, VEGF-R2 was expressed in undifferentiated monkey ES cells (day 0), but disappeared during a 4-day differentiation on OP9 feeder layer, and then reappeared after 8 days of differentiation. VEcadherin$^+$ cells appeared at day 10 of differentiation. Alkaline phosphatase activity, which was reported to be detected in undifferentiated ES cells[3,5] but not in mature vascular cells, was clearly detected in undifferentiated ES cells but not in the cells that were cultured for 8 days on an OP9 feeder layer (Figure 1C and 1D), indicating that VEGF-R2$^+$ cells at 8-day differentiation are apparently distinct from those observed in undifferentiated ES cells.

VEGF-R2$^+$ VEcadherin$^-$ cells were purified by flow cytometry sorting at day 8 (Figure 1A). Additional 5-day culturing of VEGF-R2$^+$ VEcadherin$^-$ cells on an OP9 feeder layer resulted in the appearance of PECAM1$^+$ cells (Figure 2A), which were also positive for VEcadherin and eNOS (Figure 2B and 2C). On the other hand, on a collagen IV-coated dish with 10% FCS, more than 90% of VEGF-R2$^+$ VEcadherin$^-$ cells became positive for SMA (Figure 2D) and calponin (Figure 2E) after an additional 5 days of culturing. Some were positive for SMMHC (Figure 2F). In this culturing condition, PECAM1$^+$ endothelial cells did not appear. In contrast, addition of 50ng/mL VEGF to culture on a collagen IV-coated dish resulted in the appearance of PECAM1$^+$ cells (about 20% of total cells) that were surrounded by SMA$^+$ cells (Figure 2G). VEGF-R2$^+$ VEcadherin$^-$ cells at day 10 also could differentiate into endothelial cells and mural cells similarly to day 8. VEGF-R2$^+$ VEcadherin$^-$ cells doubled themselves in about 44 hours on a collagen IV-coated dish with VEGF and FCS. Almost all of the VEGF-R2$^+$ VEcadherin$^+$ cells obtained by flow cytometry sorting at day 10 became positive for PECAM1 after an additional 5 days of culturing on a collagen IV-coated dish with 10% FCS.

We further examined whether VEGF-R2$^+$ cells can form vascular structure in vitro. Aggregates of several hundred VEGF-R2$^+$ cells were cultivated in collagen I-A gels with 10% FCS, 50ng/mL VEGF, 50ng/mL basic fibroblast growth factor, and 100 pM phorbol myristate acetate. The cells migrated out from the aggregates and formed cord-like structures within 3 days (Figure 2H).

Discussion

In the previous study,[1] we showed that VEGF-R2$^+$ cells in 4-day differentiation of mouse ES cells can differentiate into 2 major vascular cell types (endothelial cells and mural cells) in vitro and in vivo. Unlike mouse ES cells, undifferentiated monkey ES cells were already expressing VEGF-R2, similar to human ES cells. VEGF-R2 expression on monkey ES cells disappeared during 4-day differentiation on an OP9 feeder layer, and then re-expressed after 8 days of differentiation (Figure 1C). VEGF-R2–expressing cells on day 8 were different from VEGF-R2$^+$ undifferentiated monkey ES cells. First, the former did not show alkaline phosphatase activity as the latter did. Second, the former could differentiate into endothelial cells but the latter could not. Thus, the VEGF-R2$^+$ cells that re-appeared at 8 days of differentiation in monkey ES cell differentiation seem to possess similar differentiation potentials to those in 4-day differentiation of mouse ES cells,

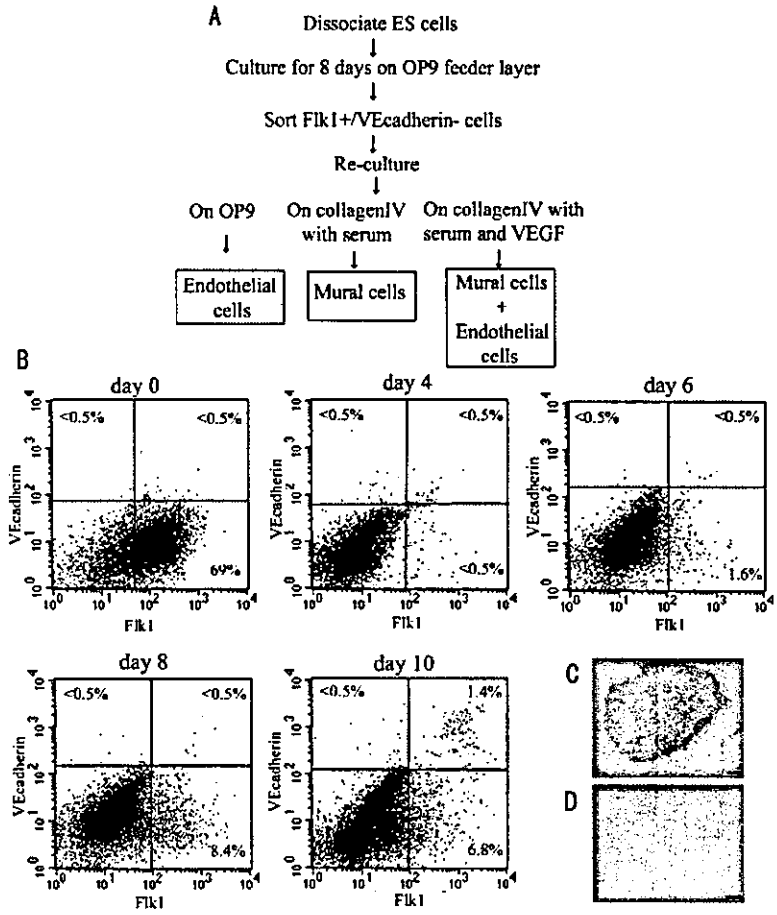

Figure 1. A, Schematic representation of the differentiation from ES cells to endothelial cells and mural cells. B, Flow cytometric analysis of the time course of differentiation of primate ES cells on an OP9 feeder layer. C, Alkaline phosphatase activity of undifferentiated ES cells on mouse embryonic fibroblast layer. D, Alkaline phosphatase activity of ES cells differentiated for 8 days on an OP9 feeder layer. Flk1 is a VEGF-R2. Scale bars: 100 μM.

whereas VEGF-R2 expression in undifferentiated monkey ES cells should be of less functional significance in vascular differentiation.

In the present study, we demonstrated that VEGF-R2$^+$ VEcadherin$^-$ cells that appeared at 8-days' differentiation in monkey ES cells give rise to both endothelial cells and mural cells and form vascular-like structures in a 3-dimentional culture in vitro. Our findings indicate that differentiated VEGF-R2$^+$ cells can act as VPCs in primates, and the differentiation kinetics of VPCs in primate and mouse ES cells were different. Thus, to seek the clinical potential of VPCs for vascular regeneration and to

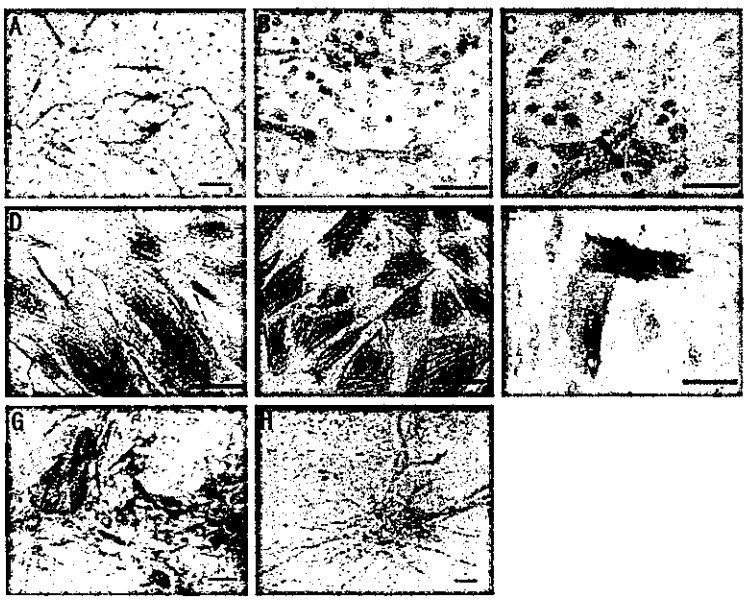

Figure 2. Immunohistochemical analysis of differentiation of primate ES cells into vascular cells (A through G). A through C, Immunostaining for endothelial cell markers: PECAM1 (A), VEcadherin (B), and eNOS (C). D through F, Immunostaining for mural cell markers: smooth muscle actin (D), calponin (E), and smooth muscle myosin heavy chain (F). G, Double immunostaining for PECAM1 (brown) and smooth muscle actin (blue). H, Tube formation of VEGF-R2$^+$ cell aggregates in 3-dimensional culture. Scale bars: B through G, 50 μM; A and H, 100 μM.

obtain novel insights in primate vascular development, investigations of primate ES cells are indispensable. Our novel in vitro vascular differentiation system using VPCs derived from primate ES cells is promising for dissecting the molecular and cellular mechanisms in the primate vascular development, to which the knock-out animal research approach is not available.

References

1. Yamashita J, Itoh H, Hirashima M, et al. Flk1-positive cells derived from embryonic stem cells serve as vascular progenitors. *Nature.* 2000;408: 92–96.
2. Yurugi-Kobayashi T, Itoh H, Yamashita J, et al. Effective contribution of transplanted vascular progenitor cells derived from embryonic stem cells to adult neovascularization in proper differentiation stage. *Blood.* 2003; 101:2675–2678.
3. Thomson JA, Kalishman J, Golos TG, et al. Isolation of a primate embryonic stem cell line. *Proc Natl Acad Sci U S A.* 1995;92:7844–7848.
4. Thomson JA, Itskovitz-Eldor J, Shapiro SS, et al. Embryonic stem cell lines derived from human blastocysts. *Science.* 1998;282:1145–1147.
5. Reubinoff BE, Pera MF, Fong CY, et al. Embryonic stem cell lines from human blastocysts: somatic differentiation in vitro. *Nat Biotechnol.* 2000; 18:399–404.
6. Suemori H, Tada T, Torii R, et al. Establishment of embryonic stem cell lines from cynomolgus monkey blastocysts produced by IVF or ICSI. *Dev Dyn.* 2001;222:273–279.
7. Amit M, Carpenter MK, Inokuma MS, et al. Clonally derived human embryonic stem cell lines maintain pluripotency and proliferative potential for prolonged periods of culture. *Dev Biol.* 2000;227:271–278.
8. Kaufman DS, Hanson ET, Lewis RL, et al. Hematopoietic colony-forming cells derived from human embryonic stem cells. *Proc Natl Acad Sci U S A.* 2001;98:10716–10721.
9. Levenberg S, Golub JS, Amit M, et al. Endothelial cells derived from human embryonic stem cells. *Proc Natl Acad Sci U S A.* 2002;99: 4391–4396.
10. Nishikawa SI, Nishikawa S, Hirashima M, et al. Progressive lineage analysis by cell sorting and culture identifies FLK1+VE-cadherin+ cells at a diverging point of endothelial and hemopoietic lineages. *Development.* 1998;125:1747–1757.
11. Hirashima M, Kataoka H, Nishikawa S, et al. Maturation of embryonic stem cells into endothelial cells in an in vitro model of vasculogenesis. *Blood.* 1999;93:1253–1263.
12. Kawasaki H, Suemori H, Mizuseki K, et al. Generation of dopaminergic neurons and pigmented epithelia from primate ES cells by stromal cell-derived inducing activity. *Proc Natl Acad Sci U S A.* 2002;99: 1580–1585.
13. Kodama H, Nose M, Niida S, et al. Involvement of the c-kit receptor in the adhesion of hematopoietic stem cells to stromal cells. *Exp Hematol.* 1994;22:979–984.
14. Kodama H, Nose M, Yamaguchi Y, et al. In vitro proliferation of primitive hemopoietic stem cells supported by stromal cells: evidence for the presence of a mechanism(s) other than that involving c-kit receptor and its ligand. *J Exp Med.* 1992;176:351–361.
15. Sawano A, Iwai S, Sakurai Y, et al. Flt-1, vascular endothelial growth factor receptor 1, is a novel cell surface marker for the lineage of monocyte-macrophages in humans. *Blood.* 2001;97:785–791.